**TABLE 3.** Relation Between Demographic and Clinical Factors and the Presence of Transmitted Drug Resistance

| | With TDR (n = 58) | Without TDR (n = 1331) | Odds Ratio* | 95% CI | *P* Value |
|---|---|---|---|---|---|
| Male gender, n (%) | 42 | 831 | 1.58 | 0.88 to 2.53 | 0.13 |
| Age (yrs), n (%) | | | | | |
| <30 | 24 | 538 | 1.00 | | |
| 30–39 | 22 | 557 | 0.98 | 0.54 to 1.78 | 0.95 |
| ≥40 | 12 | 178 | 1.67 | 0.82 to 3.42 | 0.16 |
| Time since HIV diagnosis, n (%) | | | | | |
| <6 mo | 46 | 923 | 1.00 | | |
| ≥6 mo | 12 | 401 | 0.60 | 0.31 to 1.15 | 0.12 |
| Unknown | 0 | 7 | | | |
| Year of HIV diagnosis | | | | | |
| Before 2008 | 2 | 132 | 1.00 | | |
| 2008 | 6 | 223 | 1.78 | 0.35 to 8.93 | 0.49 |
| 2009 | 13 | 301 | 2.85 | 0.63 to 12.8 | 0.17 |
| 2010 | 17 | 293 | 3.83 | 0.87 to 16.8 | 0.08 |
| 2011 | 8 | 149 | 3.54 | 0.74 to 17.0 | 0.11 |
| 2012 | 12 | 226 | 3.50 | 0.77 to 15.9 | 0.10 |
| Unknown | 0 | 7 | | | |
| Year of study enrollment, n (%) | | | | | |
| 2008 | 7 | 285 | 1.00 | | |
| 2009 | 13 | 237 | 2.23 | 0.88 to 5.69 | 0.09 |
| 2010 | 16 | 276 | 2.36 | 0.96 to 5.83 | 0.06 |
| 2011 | 8 | 286 | 1.14 | 0.40 to 3.18 | 0.80 |
| 2012 | 14 | 247 | 2.31 | 0.92 to 5.81 | 0.08 |
| Risk of HIV transmission, n (%) | | | | | |
| Heterosexual contact | 30 | 883 | 0.60 | 0.33 to 1.09 | 0.05 |
| Injection drug use | 19 | 367 | 1.49 | 0.82 to 2.69 | 0.19 |
| Other | 1 | 20 | 1.19 | 0.16 to 9.07 | 0.86 |
| Unknown | 10 | 131 | | | |
| HBs antigen positive, n (%) | 12 | 205 | 1.43 | 0.74 to 2.74 | 0.28 |
| HCV antibody positive, n (%) | 19 | 533 | 0.72 | 0.41 to 1.27 | 0.26 |
| CD4 cell count, cells/μl | | | | | |
| ≥100 | 24 | 686 | 1.00 | | |
| <100 | 34 | 642 | 1.51 | 0.89 to 2.58 | 0.14 |
| Unavailable | 0 | 3 | | | |

*Logistic regression model was used for calculating odds ratio.
CI, confidence interval.

found in our study between TDR and various risk factors, the odds ratio was lowest for heterosexual contact, with a marginal *P* value of 0.05, which indirectly suggests that other risk groups, such as IDU or men who have sex with men, is at higher risk of TDR. Meanwhile, the proportion of IDUs in our study had decreased during the 5 years along with the nationwide shift from the concentrated HIV epidemic in male IDUs to the general population. Although we failed to find the statistical impact of HIV risk group on TDR prevalence, TDR prevalence among IDU were

**TABLE 4.** Prevalence of Transmitted Drug Resistance Mutations in Specific HIV Risk Categories

| | Total | 2008 | 2009 | 2010 | 2011 | 2012 |
|---|---|---|---|---|---|---|
| Total TDR rate [% (n/total)] | 4.18 (58/1389) | 2.40 (7/292) | 5.20 (13/250) | 5.48 (16/292) | 2.72 (8/294) | 5.36 (14/261) |
| TDR rate in HIV risk categories [% (n/total)] | | | | | | |
| Heterosexual contact alone | 3.33 (28/840) | 1.40 (2/143) | 4.90 (7/143) | 3.40 (5/147) | 1.92 (4/208) | 5.02 (10/199) |
| IDU alone | 5.41 (17/314) | 4.10 (3/73) | 5.88 (4/68) | 6.67 (6/90) | 2.27 (1/44) | 7.69 (3/39) |
| IDU plus heterosexual | 2.78 (2/72) | 3.45 (1/29) | 0 (0/5) | 0 (0/3) | 3.57 (1/28) | 0 (0/7) |
| Homosexual contact alone | 0 (0/2) | 0 (0/2) | - (0/0) | - (0/0) | - (0/0) | - (0/0) |
| Other | 0 (0/20) | 0 (0/13) | 0 (0/3) | 0 (0/1) | 0 (0/3) | - (0/0) |
| Unknown | 7.80 (11/141) | 3.13 (1/32) | 6.45 (2/31) | 9.80 (5/51) | 18.2 (2/11) | 6.25 (1/16) |

**TABLE 5.** Characteristics of 4 Patients With Drug Resistance Mutations Against Multiple Class Antiretrovirals

| Patient ID | Year of HIV Diagnosis | Year of Study Participant | Sex | Risk of HIV Infection | CD4 Count (Cells/μL) | HIV-RNA (Log Copies/mL) | HBs Antigen | HCV Antibody | Resistance Mutations | |
|---|---|---|---|---|---|---|---|---|---|---|
| | | | | | | | | | NRTI | NNRTI |
| 08HT0059 | 2003 | 2008 | M | Heterosexual | 10 | 4.11 | Negative | Negative | L74V | V106I, G190A |
| 10HT0136 | 2010 | 2010 | F | Unknown | 283 | 4.60 | Negative | Negative | D67E | Y188C |
| 11HT0201 | 2011 | 2011 | F | Heterosexual | 272 | 5.98 | Positive | Negative | M41L, M184V, T215Y | Y181C, G190A |
| 11HT0299 | 2011 | 2011 | M | Unknown | 147 | 5.83 | Negative | Negative | M184V | V106I, V179D, Y188L |

relatively higher, which was above 5% in 2009, 2010, and 2012 and had changed along with the overall TDR prevalence. These findings support that IDU is still important as a TDR risk factor in this population. In this regard, however, our study enrolled 141 patients who were free of possible HIV risk or refused to provide information on their risky behavior. Because their TDR prevalence was high over the study period, their concealment of IDU experience could influence the analysis. Although our study was conducted only in urban area, our findings in individuals at most risk of TDR are useful for the assessment of the situation in the near future of the entire HIV population in Vietnam, including rural area where ART has been rapidly distributed in recent years.

With respect to the drug class, the TDR prevalence was 2.02% for NRTI, 1.37% for NNRTI, and 1.08% for PI. Compared with the TDR rate for CRF01_AE strain in the TDR lists for surveillance[18] (2.9% for NRTI, 0.5% for NNRTI, and 1.5% for PI), the TDR prevalence of NNRTI-related mutations was higher for the entire study period and considered to have increased with ART scale-up. The Vietnamese national guideline for ART recommended nevirapine as one of the first-line regimen in 2005 and either nevirapine and efavirenz since 2009,[6–8] and generally NNRTI-base regimens have low genetic barriers for development of drug resistance. This background provides reasonable explanation of frequent detection of NNRTI-related mutations like in other resource-limited countries. However, TAMs and M184V or I were predominantly seen in NRTI-related mutations, which have clinically significant impact on treatment outcome. Even after changing the first-line NRTI in the national ART guideline from zidovudine (AZT) or stavudine (d4T) into tenofovir (TDF) in 2010, AZT or d4T were still extensively used in Vietnam over the study period. In Western Europe, a decline in the prevalence of TAMs is being observed in treatment-experienced cohort as a consequence of changing prescription patterns and prompt management of treatment failure.[25,26] Therefore, the TDR patterns in Vietnam could be changed with future increase in TDF use and decrease in AZT or d4T use. We should note that 4 individuals in our study had TDR in multiple drug classes, including 1 who had very extensive resistance: M41L, M184V, T215Y in NRTI and Y181C and G190A in NNRTI, which strongly compromise the efficacy of the first-line regimens in Vietnam and could threaten the nationwide ART scale-up program if it spreads. There are multiple factors that influence the prevalence of individual resistance mutations in primary HIV drug resistance but treatment-experienced persons with resistance might be the main source of such multiple-class TDR. Although continuous TDR surveillance is important to catch TDR expansion, efforts to enhance early diagnosis of treatment failure with improvement in availability of tests for plasma viral load and drug resistance in individuals on treatment, should be encouraged to prevent transmission of drug-resistant HIV.

In conclusion, TDR prevalence in Southern Vietnam remained low during the rapid scale-up of ART in 2008–2012. No demographic factor was statistically related to TDR detection, and the patterns of detected TDRs were similar to those described in previous reports. Although the average TDR prevalence was low, moderate prevalence was noted in part of the study period, and multiple-class TDR was detected in some patients. Because ART will continue to be scaled up, the TDR rate can rise in the future. Our results highlight the importance of TDR surveillance over a long period of time to provide proper assessment of the ART scale-up program.

## ACKNOWLEDGMENTS

*The authors thank Do Thi Cam Nhung for collecting the blood specimens, Keiko Saito, and Nguyen Thi Huyen for their assistance in study operation.*

## REFERENCES

1. National Committee for AIDS, Drug and Prostitution Prevention and Control, Ministry of Health, Socialist Republic of Viet Nam. *Viet Nam AIDS Response Progress Report 2012*. 2012. Available at: http://www.unaids.org/en/dataanalysis/knowyourresponse/countryprogressreports/2010countries/vietnam_2010_country_progress_report_en.pdf. Accessed September 30, 2013.
2. Gupta RK, Jordan MR, Sultan BJ, et al. Global trends in antiretroviral resistance in treatment-naive individuals with HIV after rollout of antiretroviral treatment in resource-limited settings: a global collaborative study and meta-regression analysis. *Lancet*. 2012;380:1250–1258.
3. Bennett DE, Bertagnolio S, Sutherland D, et al. The World Health Organization's global strategy for prevention and assessment of HIV drug resistance. *Antivir Ther*. 2008;13(suppl 2):1–13.
4. Jordan MR, Bennett DE, Wainberg MA, et al. Update on World Health Organization HIV drug resistance prevention and assessment strategy: 2004-2011. *Clin Infect Dis*. 2012;54:S245–S249.
5. Socialist Republic of Viet Nam. *Vietnam Country Progress Report 2010 on the Declaration of Commitment on HIV/AIDS, Adopted at the 26th United Nations General Assembly Special Session in 2001 (UNGASS)*. 2010. Available at: http://www.unaids.org/en/dataanalysis/knowyourresponse/countryprogressreports/2010countries/vietnam_2010_country_progress_report_en.pdf. Accessed September 30, 2013.
6. Ministry of Health, Socialist Republic of Viet Nam. *Antiretroviral Treatment Protocol for People Living With HIV/AIDS*. 2006 (No: 2051/QD-BYT).

7. Ministry of Health, Socialist Republic of Viet Nam. *Guidelines for Diagnosis and Treatment of HIV/AIDS.* 2009 (No. 3003/QĐ-BYT).
8. Ministry of Health, Socialist Republic of Viet Nam. *Guidelines for Diagnosis and Treatment of HIV/AIDS.* 2011 (No: 4139/QĐ-BYT).
9. The World Health Organization. *Consolidated Guidelines on the Use of Antiretroviral Drugs for Treating and Preventing HIV Infection: Recommendations for a Public Health Approach.* Geneva: WHO; 2013. Available at: http://www.who.about/licensing/copyright_form/en/index.html. Accessed September 30, 2013.
10. Lan NT, Recordon-Pinson P, Hung PV, et al. HIV type 1 isolates from 200 untreated individuals in Ho Chi Minh City (Vietnam): ANRS 1257 Study. Large predominance of CRF01_AE and presence of major resistance mutations to antiretroviral drugs. *AIDS Res Hum Retroviruses.* 2003;19:925–928.
11. Nguyen HT, Duc NB, Shrivastava R, et al. HIV drug resistance threshold survey using specimens from voluntary counseling and testing sites in Hanoi, Vietnam. *Antivir Ther.* 2008;13:115–121.
12. Duc NB, Hien BT, Wagar N, et al. Surveillance of transmitted HIV drug resistance using matched plasma and dried blood spot specimens from voluntary counseling and testing sites in Ho Chi Minh City, Vietnam, 2007-2008. *Clin Infect Dis.* 2012;54:S343–S347.
13. Tran VT, Ishizaki A, Nguyen CH, et al. No increase of drug-resistant HIV type 1 prevalence among drug-naive individuals in Northern Vietnam. *AIDS Res Hum Retroviruses.* 2012;28:1349–1351.
14. Dean J, Ta Thi TH, Dunford L, et al. Prevalence of HIV type 1 antiretroviral drug resistance mutations in Vietnam: a multicenter study. *AIDS Res Hum Retroviruses.* 2011;27:797–801.
15. Ayouba A, Lien TT, Nouhin J, et al. Low prevalence of HIV type 1 drug resistance mutations in untreated, recently infected patients from Burkina Faso, Côte d'Ivoire, Senegal, Thailand, and Vietnam: the ANRS 12134 study. *AIDS Res Hum Retroviruses.* 2009;25:1193–1196.
16. Bontell I, Cuong do D, Agneskog E, et al. Transmitted drug resistance and phylogenetic analysis of HIV CRF01_AE in Northern Vietnam. *Infect Genet Evo.* 2012;12:448–452.
17. Do TN, Nguyen TM, Do MH, et al. Combining cohort analysis and monitoring of HIV early-warning indicators of drug resistance to assess antiretroviral therapy services in Vietnam. *Clin Infect Dis.* 2012;54:S306–S312.
18. Bennett DE, Camacho RJ, Otelea D, et al. Drug resistance mutations for surveillance of transmitted HIV-1 drug-resistance: 2009 update. *PLoS One.* 2009;4:e4724.
19. Ariyoshi K, Matsuda M, Miura H, et al. Patterns of point mutations associated with antiretroviral drug treatment failure in CRF01_AE (subtype E) infection differ from subtype B infection. *J Acquir Immune Defic Syndr.* 2003;33:336–342.
20. Stanford HIV Drug Resistance Database. *Mutation Prevalence According to Subtype and Treatment.* Stanford, CA: Stanford University. Available at: http://hivdb.stanford.edu/cgi-bin/MutPrevBySubtypeRx.cgi. Accessed July 1, 2013.
21. Johnson VA, Calvez V, Gunthard HF, et al. Update of the drug resistance mutations in HIV-1: 2013. *Top Antivir Med.* 2013;21:6–14.
22. Paredes R, Sagar M, Marconi VC, et al. In vivo fitness cost of the M184V mutation in multidrug-resistant human immunodeficiency virus type 1 in the absence of lamivudine. *J Virol.* 2009;83:2038–2043.
23. Weber R, Huber M, Rickenbach M, et al. Uptake of and virological response to antiretroviral therapy among HIV-infected former and current injecting drug users and persons in an opiate substitution treatment programme: the Swiss HIV Cohort Study. *HIV Med.* 2009;10:407–416.
24. Werb D, Mills EJ, Montaner JS, et al. Risk of resistance to highly active antiretroviral therapy among HIV-positive injecting drug users: a meta-analysis. *Lancet Infect Dis.* 2010;10:464–469.
25. Cane P, Chrystie I, Dunn D, et al. UK Group on Transmitted HIV Drug Resistance. Time trends in primary resistance to HIV drugs in the United Kingdom: multicentre observational study. *Br Med J.* 2005;331:1368–1374.
26. Payne BA, Nsutebu EF, Hunter ER, et al. Low prevalence of transmitted antiretroviral drug resistance in a large UK HIV-1 cohort. *J Antimicrob Chemother.* 2008;62:464–468.

Peptide Antivirals Hot Paper

DOI: 10.1002/anie.201404684

# Cell-Penetrating, Dimeric α-Helical Peptides: Nanomolar Inhibitors of HIV-1 Transcription**

*Sangmok Jang, Soonsil Hyun, Seoyeon Kim, Seonju Lee, Im-Soon Lee, Masanori Baba, Yan Lee,* and Jaehoon Yu**

***Abstract:*** *We constructed dimeric α-helical peptide bundles based on leucine (L) and lysine (K) residues for both efficient cell penetration and inhibition of the Tat–TAR interaction. The LK dimers can penetrate nearly quantitatively into eukaryotic cells and effectively inhibit the elongation of the TAR transcript at low nanomolar concentrations. The effective inhibition of HIV-1 replication strongly suggests that the LK dimer has strong potential as an anti-HIV-1 drug.*

RNA structure is used as a control element in most biological systems.[1] Human immunodeficiency virus-1 (HIV-1) contains a short hairpin RNA, named TAR, located in the long terminal repeat (LTR) region that participates in efficient transcription of the integrated genome.[2] Specifically, the interaction between TAR RNA and the viral Tat protein activates the transcription of viral genes.[2b–d,3] Consequently, this interaction is a plausible target when developing substances that destroy HIV-1.[4] However, no pharmaceutical agents that inhibit Tat binding to hairpin RNA proteins have been commercialized thus far. The likely reason for this lies in the fact that small molecules that can penetrate cells[5] bind ineffectively to TAR and the poor cell-penetrating ability of large molecules that efficiently inhibit the Tat–TAR interaction.[6]

Peptides are attractive biomaterials that can be employed to inhibit the Tat–TAR interaction. Thus, Tat-derived peptide fragments, as well as cyclized and more extended analogues of Tat, have been explored to assess their competitive binding affinities against hairpin RNA.[7] Members of a recently updated list of such peptides were shown to possess single-digit nanomolar affinities against TAR,[8] which suggests that they are potential candidates as therapeutic drugs to target HIV-1. However, although Tat is a well-known cell-penetrating peptide (CPP),[9] the cell permeabilities of Tat analogues are insufficiently low when in-cell concentrations in the nanomolar range are required. As a result of the weak cell-penetrating activities of these peptides, significant differences exist between the dissociation constants ($K_d$) arising from in vitro binding and cell-based assays.

Recently, we observed that a strong correlation exits between the α helicities and the cell-penetrating activities of amphipathic peptides composed of leucine (L) and lysine (K) residues. Furthermore, we constructed dimeric bundle amphipathic peptides containing two cysteine residues per monomer as replacements for the leucine residues located at the $i$ and $i+7$ positions on the hydrophobic face as well as two disulfide bonds connecting the cysteine residues.[8a] Compared to their monomeric counterparts, the dimeric peptides display higher α helicities as well as stronger affinities (corresponding to sub-nanomolar $K_d$ values) against hairpin RNA targets. In addition, the amphipathic characteristics and high α helicities of the dimeric peptides lead to high cell-penetrating activities and, consequently, the peptides can serve as effective intracellular inhibitors of HIV-1 transcription in mammalian cells (Figure 1). Their high cell penetration and TAR RNA binding abilities not only make these peptides the first agents that inhibit transcription of the integrated HIV-1 genome, but also the first peptides that serve as key leads in the search for drugs for the treatment of HIV-1.

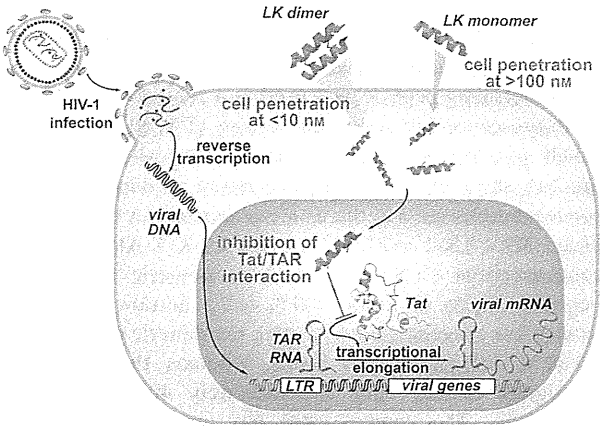


***Figure 1.*** Schematic representation of the inhibition of Tat-TAR-mediated transactivation by using LK peptides.

[*] S. Jang,[+] S. Lee, Prof. Dr. Y. Lee
Department of Chemistry, Seoul National University
Seoul 151-742 (Korea)
E-mail: gacn@snu.ac.kr
Dr. S. Hyun,[+] S. Kim, Prof. Dr. J. Yu
Department of Chemistry & Education, Seoul National University
Seoul 151-742 (Korea)
E-mail: jhoonyu@snu.ac.kr
Prof. Dr. I.-S. Lee
Department of Biological Sciences, Konkuk University
Seoul 143-701 (Korea)
Prof. Dr. M. Baba
Graduate School of Medical and Dental Sciences
Kagoshima University
Kagoshima 890-8580 (Japan)
[+] These authors contributed equally to this work.

[**] This work was supported by the Mid-career Researcher Program (2011-0013569 and 2013064805) funded by the Ministry of Science, ICT, and Future Planning, Korea.
Supporting information for this article is available on the WWW under http://dx.doi.org/10.1002/anie.201404684.

  

*Table 1:* Binding affinities on TAR RNA and α helicities of LK peptides[a]

| Peptide | Sequences of peptide[b] | $K_d$ [nM] | α helicity [%][d] |
|---|---|---|---|
| LK-1 | LKKLLKLLKKLLKLAG | 63[c] | 24/77 |
| LK-2 | LKKLCKLLKKLCKLAG | 9.6[c] | 28/77 |
| LK-3 | LKKLCKLLKKLCKLAG<br>LKKLCKLLKKLCKLAG | 0.061[c] | 91/99 |
| LK-4 | LKKLCKLLKKLCKLAG<br>LKKLCKLLKKLCKLAG | 0.059 | 87/92 |
| R9 | RRRRRRRRR | n.d.[e] | 13/15 |

[a] Affinities were measured at 20 °C by fluorescence anisotropy using the rhodamine-Rev peptide as a probe. [b] Disulfide linkers are shown in dotted lines in LK-3. *N,N'*-Phenylenedimaleimide linkers are shown in solid lines in LK-4. N-terminal and C-terminal modification of all peptides were performed with acetylation (Ac) and amidation ($NH_2$), respectively. [c] Data are adopted from a previous report.[8a] [d] The α helicities of peptides were measured by circular dichroism (CD) in PBS (pH 7.4; the first value) and in 50% TFE in the same buffer (the second value). [e] n.d.: not determined.

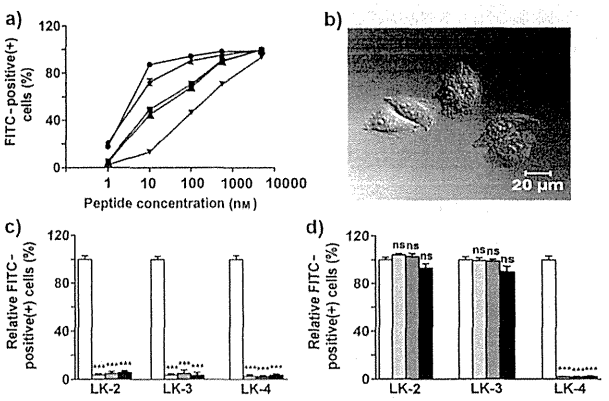


*Figure 2.* Cell-penetration activity of the LK peptides on HeLa cells after 12 h incubation. a) FACS results for LK-1 (▲), LK-2 (■), LK-3 (●), LK-4 (◆), and R9 (▼) at various peptide concentrations. b) Confocal laser scanning microscopy (CLSM) images of HeLa cells with FITC-labeled LK-3 (10 nM). The nucleus was stained with Hoechst 33442 (blue). c,d) The relative cell-penetration activity of the LK peptides at endocytosis-inhibiting conditions at 10 nM (c) and 500 nM (d). Control (white), wortmannin (gray), amiloride (dark gray), and 4 °C (black). Each error bar represents the standard deviation ($n=3$). The markers (***) and (n.s.) indicate $p<0.001$ and no significant difference compared with the control, respectively.

The current investigation arose from an earlier observation[8] that the peptide LKKLLKLLKKLLKLAG (LK-1, Table 1) has a strong binding affinity to short hairpin RNAs. In addition, we found that the amphipathic head-to-head dimeric bundle LK-3,[8a] which contains two disulfide bonds in the middle of each chain, has a sub-nanomolar affinity to TAR RNA. LK-1 and LK-3 were selected for our continuing studies aimed at the development of anti-HIV-1 peptides. As the disulfide bonds in LK-3 might be cleaved under cytosolic conditions,[8a,10] the reduced monomeric peptide (LK-2) was generated for use as a control. Furthermore, the nonreducible dimer (LK-4), in which the peptide chains are linked by two *N,N'*-phenylenedimaleimide moieties, was also prepared. Inspection of the dissociation constants ($K_d$) for the binding of the LK peptides to TAR RNA (Table 1) shows that LK-3 and LK-4 display about 100 and 1000 times stronger affinities than the monomeric peptides LK-1 and LK-2. In addition, we determined the α helicities of the LK peptides in phosphate-buffered saline (PBS; pH 7.4) under membrane-mimic conditions (50% trifluoroethanol (TFE) in the PBS). The data show that the dimeric peptides have significantly higher α helicities (about 90%) than their monomeric counterparts.

The ability of the monomeric and dimeric peptides to penetrate mammalian cells was evaluated next. For this purpose, LK peptides labeled with fluorescein isothocyanate (FITC) were incubated with HeLa cells. R9, a well-known cell-penetrating peptide, was used as a control.[11] The results of fluorescence-activated cell sorting (FACS) experiments, which give the percentage of the FITC-positive cells (Figure 2a), show that the cell-penetration activities at all the concentrations used in the analysis increase in the following order: R9 < LK-1 and LK-2 < LK-4 < LK-3. At high peptide concentrations (> 500 nM), both monomeric and dimeric peptides display an almost 100% cell penetration. However, at very low concentrations (10 nM), the dimeric peptides have 70–90% cell-penetration levels, whereas the monomeric analogues display only approximately 40% penetration efficiencies. The control (R9) has only a minimal cell-penetration activity at 10 nM. The combined observations demonstrate that the cell-penetrating abilities of the LK peptides are greatly improved by the formation of dimers. Significant portions of the LK peptides are delivered into cell nuclei (Figure 2b, see also Figures S4 and S5 in the Supporting Information). The dimeric LK peptides also have greatly improved penetration abilities in a mouse leukemic monocyte macrophage cell line (RAW 264.7; see Figure S3 in the Supporting Information).

The cell permeabilities of the LK peptides were examined under various endocytosis-inhibiting conditions. The results show that the mechanism employed is dependent on the peptide concentration. At low concentrations (10 nM), the cell-penetration abilities of all the LK peptides are nearly completely inhibited by lowering the temperature to 4 °C or by treatment with endocytosis inhibitors (wortmannin or amiloride; Figure 2c).[12] Thus, it appears that at low concentrations, LK peptides are internalized by cells through energy-dependent endocytic pathways, even though the activities of each LK peptide differs significantly at these concentrations. At high concentrations (500 nM), where all the LK peptides display > 80% cellular uptake, the cell-penetration mechanism varies (Figure 2d). For example, wortmannin and amiloride display almost no inhibition of cell penetration by both monomeric LK-2 and dimeric LK-3, and the internalization efficiencies of these peptides remain unchanged even at 4 °C. Thus, LK-2 and LK-3 penetrate into cells through an energy-independent pathway at high concentrations, not by receptor-mediated endocytosis or macropinocytosis. Interestingly, cell penetration by the 500 nM dimer LK-4, which contains nonreducible maleimide linkers in place of the disulfides, is nearly completely inhibited by lowering the temperature or by treatment with either endocytosis inhibitor. The results suggest that LK-2 or LK-3 undergo energy-independent cell penetration (e.g. hole or carpet formation)[13] at high concentrations, but LK-4 undergoes energy-

  

dependent cell penetration because of the structural difference.

Since they can be delivered into cells at nanomolar concentrations, the LK peptides were employed in experiments to determine if they inhibit the viral target inside host cells. A reporter system was constructed on HeLa cells by co-transfection with pLTR-luc, a plasmid containing an HIV-1 LTR promoter and a firefly luciferase gene, as well as pTat, a plasmid-containing HIV-1 Tat gene.[14] In this system, expressed Tat proteins should interact with TAR RNA in the LTR promoter as an anti-termination factor to promote transcription of the luciferase gene. After 12 h incubation of the reporter cells with the LK peptides, the relative amounts of mRNA were determined by using RT-PCR (Figure 3). The results show that, compared with those of the two house-

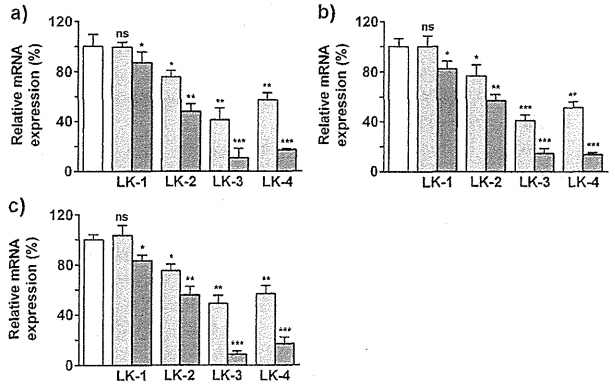


*Figure 3.* Inhibition of the Tat-mediated transcriptional elongation by LK peptides in HeLa cells. Relative mRNA expression of a) TAR-luc/β-actin, b) TAR-luc/18S rRNA, and c) TAR-luc/TAR at 10 nM and 100 nM of each LK peptide. Control (white), 10 nM (gray), 100 nM (dark gray). Each error bar represents the standard deviation ($n=3$). The markers (*), (**), (***), and (n.s.) indicate $0.01 \le p < 0.1$, $0.001 \le p < 0.01$, $p < 0.001$, and no significant difference compared with the control, respectively.

keeping genes β-actin and 18S rRNA, the amounts of mRNA in the luciferase gene decreases in a peptide dose dependent manner (Figure 3a,b). Moreover, the amount of the long luciferase gene transcript with total TAR RNA transcribed was evaluated to demonstrate that the LK peptides do not prevent transcription by binding to transfected plasmid DNA. The ratio of TAR-luc (long transcript) to TAR (total transcript) was found to be similar to the ratio of TAR-luc to mRNA in the house-keeping genes. This observation suggests that the Tat–TAR interaction is inhibited by the LK peptides at the transcriptional elongation level (Figure 3c).

The inhibitory activity against Tat-mediated transcription varies among the peptides, with monomeric LK-1 and LK-2 exhibiting less than 50% inhibition even at 100 nM. In contrast, dimeric peptides LK-3 and LK-4, which possess higher cell-penetration abilities, display about 50% inhibition at 10 nM, and more than 80% inhibition at 100 nM. As the HeLa cell penetration activities of LK-1 and LK-2 are similar (Figure 2a), the stronger inhibitory effect of LK-2 is likely a consequence of its stronger binding affinity to TAR RNA (Table 1). As disulfide bonds are readily degraded under reductive cytosolic conditions, it is likely that, after internalization, LK-3 is reduced in the cytosol to form monomeric LK-2, which still binds to the TAR RNA with nanomolar affinity. Therefore, the enhanced cell-penetration activity of LK-3 over LK-2 is the main source of its outstanding ability to inhibit the Tat–TAR interaction at the transcriptional level. Although its cell-penetration ability is slightly less than that of LK-3, LK-4 displays a similar inhibitory activity as LK-3 because of the effect of the nonreducible linker that enables the peptide to retain its dimeric form in the cytosol and high TAR RNA binding affinity.

The $IC_{50}$ values of the LK peptides, determined by using the luciferase assay (Figure 4), were found to decrease in the order LK-1 (110 nM) > LK-2 (50 nM) > LK-4 (35 nM) > LK-3 (10 nM). The $IC_{50}$ value of dimeric LK-3, which is more than tenfold lower than that of monomeric LK-1, is a consequence of its enhanced cell-penetration ability as well as the twofold

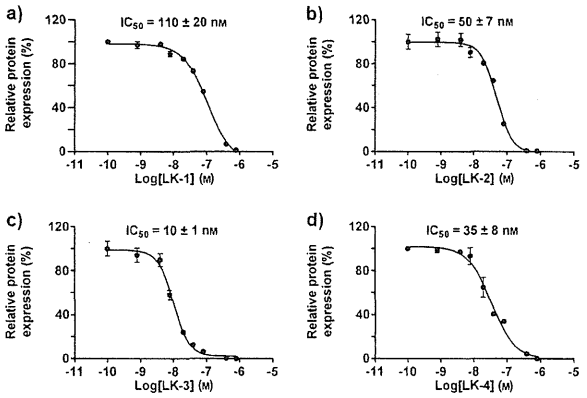


*Figure 4.* Inhibition of luciferase expression by a) LK-1, b) LK-2, c) LK-3, and d) LK-4 peptides in HeLa cells. Each error bar represents the standard deviation ($n=3$).

increase in the concentration of the monomeric peptide that takes place when LK-3 undergoes cytosolic cleavage. The $IC_{50}$ value of LK-3 is almost the same as the dissociation constant of LK-2 ($K_d = 9.6$ nM), which indicates that cell-membrane penetration no longer serves as the barrier for in-cell activity, a unique feature not shared by other peptide drugs that display large discrepancies between the $K_d$ and $IC_{50}$ values. Similar results ($IC_{50}$ of LK-3 = 18 nM) are also seen in studies using macrophage cells (RAW 264.7; see Figure S6 in the Supporting Information). Moreover, the decrease in the inhibition of the LK peptides corresponds to the increase in Tat expression (see Figure S7 in the Supporting Information). The result also suggests that the competitive binding between Tat and LK peptides on TAR RNA is the main factor for the inhibition.

The membrane destabilization and cytotoxicities of the peptides were determined by using lactate dehydrogenase (LDH) and 3-(4,5-dimethylthiazol-2-yl)-2,5-diphenyltetrazolium bromide (MTT) assays, respectively (see Figures S8 and S9 in the Supporting Information). The results demonstrate that none of the LK peptides cause membrane destabilization

  

up to 2 μM concentrations, and only LK-3 brings about a small membrane destabilization at 8 μM. Also, the MTT assay results show that LK-3 is not cytotoxic at concentrations below 10 μM, similar to the previous report on oligoarginine peptides.[15] These observations suggest that the high cell-penetrating activities of the LK peptides is not caused by disruption of the plasma membrane, which would induce cell lysis and eventually cell death.

In the final phase of this effort, the inhibitory effects of the peptides on HIV-1 replication in acutely infected T-lymphoblastoid cells (MOLT-4/CCR5)[16] were evaluated (Figure 5). The $IC_{50}$ values of LK-3 and LK-4 for HIV-1 replication were

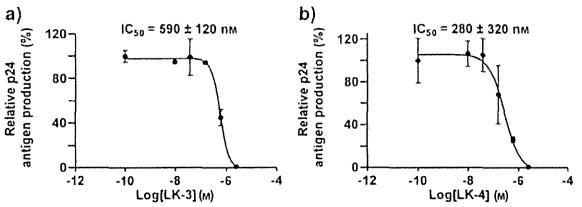


*Figure 5.* Inhibition of HIV-1 replication by a) LK-3 and b) LK-4 peptides in T-lymphoblastoid cells (MOLT-4/CCR5). Each error bar represents the standard deviation ($n=3$).

590 and 280 nM, respectively, while that of LK-1 was $>2$ μM (data not shown). The larger $IC_{50}$ values, compared with those arising from experiments with HeLa or RAW 264.7 cells, may be partially attributed to the reduced penetration activity of the peptides in T-lymphoblastoid cells. However, LK-3 did not show significant cytotoxicity to the host cells at concentrations up to 2.6 μM, which is considerably higher than its $IC_{50}$ value for HIV-1 replication. LK-4 was found to be more active than LK-3, but it was also more cytotoxic to the host cells (data not shown). These findings suggest that the LK dimers, especially LK-3, have potential as a therapeutic against HIV-1.

In summary, we have demonstrated that α-helical LK dimeric bundles have large cell-penetrating abilities and that they target intracellular hairpin RNA. Approximately 90% of the LK dimers exist in a helical form in an aqueous buffer, and hence have significantly enhanced cell-penetration activities compared to those of the corresponding monomer. This feature results in near quantitative uptake of the dimeric peptides in HeLa and macrophage cells at low nanomolar concentrations. We showed that the LK dimers display dose-dependent inhibition of the Tat–TAR interaction, with $IC_{50}$ values that are about 10 nM. In addition, the dimeric peptides are not cytotoxic at concentrations $<2$ μM. The experiments using HIV-1-infected cells show that LK-3 and LK-4 inhibit viral replication at nanomolar concentrations. This finding strongly suggests that the LK dimers have the potential to serve as effective anti-HIV-1 drugs. Target selectivity, stability, and long-term toxicity of the LK dimers will be further investigated for the future development of new anti-HIV-1 drugs based on the LK dimers.

Received: April 25, 2014
Published online: July 23, 2014

**Keywords:** antiviral agents · drug design · HIV-1 · peptides · transcriptional inhibition

[1] P. Svoboda, A. Di Cara, *Cell. Mol. Life Sci.* **2006**, *63*, 901–908.
[2] a) C. A. Rosen, J. G. Sodroski, W. A. Haseltine, *Cell* **1985**, *41*, 813–823; b) S. Y. Kao, A. F. Calman, P. A. Luciw, B. M. Peterlin, *Nature* **1987**, *330*, 489–493; c) B. Berkhout, R. H. Silverman, K. T. Jeang, *Cell* **1989**, *59*, 273–282; d) H. Lu, Z. Li, Y. Xue, Q. Zhou, *Chem. Rev.* **2013**, *113*, 8567–8582.
[3] M. F. Laspia, A. P. Rice, M. B. Mathews, *Cell* **1989**, *59*, 283–292.
[4] a) F. Darfeuille, A. Arzumanov, S. Gryaznov, M. J. Gait, C. Di Primo, J. J. Toulme, *Proc. Natl. Acad. Sci. USA* **2002**, *99*, 9709–9714; b) S. Bannwarth, A. Gatignol, *Curr. HIV Res.* **2005**, *3*, 61–71.
[5] a) O. Tabarrini, S. Massari, D. Daelemans, F. Meschini, G. Manfroni, L. Bottega, B. Gatto, M. Palumbo, C. Pannecouque, V. Cecchetti, *ChemMedChem* **2010**, *5*, 1880–1892; b) S. Massari, D. Daelemans, M. L. Barreca, A. Knezevich, S. Sabatini, V. Cecchetti, A. Marcello, C. Pannecouque, O. Tabarrini, *J. Med. Chem.* **2010**, *53*, 641–648; c) G. Manfroni, B. Gatto, O. Tabarrini, S. Sabatini, V. Cecchetti, G. Giaretta, C. Parolin, C. Del Vecchio, A. Calistri, M. Palumbo, A. Fravolini, *Bioorg. Med. Chem. Lett.* **2009**, *19*, 714–717.
[6] D. Wang, J. Iera, H. Baker, P. Hogan, R. Ptak, L. Yang, T. Hartman, R. W. Buckheit, Jr., A. Desjardins, A. Yang, P. Legault, V. Yedavalli, K. T. Jeang, D. H. Appella, *Bioorg. Med. Chem. Lett.* **2009**, *19*, 6893–6897.
[7] a) A. Davidson, T. C. Leeper, Z. Athanassiou, K. Patora-Komisarska, J. Karn, J. A. Robinson, G. Varani, *Proc. Natl. Acad. Sci. USA* **2009**, *106*, 11931–11936; b) A. Friedler, D. Friedler, N. W. Luedtke, Y. Tor, A. Loyter, C. Gilon, *J. Biol. Chem.* **2000**, *275*, 23783–23789; c) I. Huq, Y. H. Ping, N. Tamilarasu, T. M. Rana, *Biochemistry* **1999**, *38*, 5172–5177; d) F. Hamy, E. R. Felder, G. Heizmann, J. Lazdins, F. Aboul-ela, G. Varani, J. Karn, T. Klimkait, *Proc. Natl. Acad. Sci. USA* **1997**, *94*, 3548–3553.
[8] a) S. Hyun, J. Na, S. J. Lee, S. Park, J. Yu, *ChemBioChem* **2010**, *11*, 767–770; b) Y. Lee, S. Hyun, H. J. Kim, J. Yu, *Angew. Chem. Int. Ed.* **2008**, *47*, 134–137; *Angew. Chem.* **2008**, *120*, 140–143.
[9] a) A. Ziegler, P. Nervi, M. Durrenberger, J. Seelig, *Biochemistry* **2005**, *44*, 138–148; b) S. Fawell, J. Seery, Y. Daikh, C. Moore, L. L. Chen, B. Pepinsky, J. Barsoum, *Proc. Natl. Acad. Sci. USA* **1994**, *91*, 664–668; c) E. Vives, P. Brodin, B. Lebleu, *J. Biol. Chem.* **1997**, *272*, 16010–16017.
[10] a) Y. Lee, H. Koo, G. W. Jin, H. Mo, M. Y. Cho, J. Y. Park, J. S. Choi, J. S. Park, *Biomacromolecules* **2005**, *6*, 24–26; b) Y. Lee, H. Mo, H. Koo, J. Y. Park, M. Y. Cho, G. W. Jin, J. S. Park, *Bioconjugate Chem.* **2007**, *18*, 13–18.
[11] a) P. A. Wender, D. J. Mitchell, K. Pattabiraman, E. T. Pelkey, L. Steinman, J. B. Rothbard, *Proc. Natl. Acad. Sci. USA* **2000**, *97*, 13003–13008; b) P. Guterstam, F. Madani, H. Hirose, T. Takeuchi, S. Futaki, S. El Andaloussi, A. Graslund, U. Langel, *Biochim. Biophys. Acta Biomembr.* **2009**, *1788*, 2509–2517.
[12] A. El-Sayed, H. Harashima, *Mol. Ther.* **2013**, *21*, 1118–1130.
[13] H. D. Herce, A. E. Garcia, *Proc. Natl. Acad. Sci. USA* **2007**, *104*, 20805–20810.
[14] J. Pai, T. Yoon, N. D. Kim, I. S. Lee, J. Yu, I. Shin, *J. Am. Chem. Soc.* **2012**, *134*, 19287–19296.
[15] M. Kosuge, T. Takeuchi, I. Nakase, A. T. Jones, S. Futaki, *Bioconjugate Chem.* **2008**, *19*, 656–664.
[16] M. Baba, H. Miyake, M. Okamoto, Y. Iizawa, K. Okonogi, *AIDS Res. Hum. Retroviruses* **2000**, *16*, 935–941.

  

Indian J Hematol Blood Transfus (July-Sept 2014) 30(3):191–194
DOI 10.1007/s12288-014-0345-9

SHORT COMMUNICATION

# Epstein–Barr Viral Load is Associated to Response in AIDS-Related Lymphomas

**Paula Yurie Tanaka · Kouichi Ohshima · Masao Matsuoka · Ester Cerdeira Sabino · Suzete Cleusa Ferreira · Anna Shoko Nishya · Renata de Oliveira Costa · Edenilson Eduardo Calore · Nilda Maria Perez · Juliana Pereira**

Received: 27 October 2013 / Accepted: 22 January 2014 / Published online: 8 February 2014


**Abstract** AIDS-related lymphoma (ARL) development is associated to immunodeficiency state with proliferation of B-cells driven by HIV itself and EBV infection. However, Epstein–Barr DNA is not detected in malignant cells of all ARL subtypes. A prospective and controlled study to analyze EBV viral load (VL) in plasma and peripheral blood mononuclear cells (PBMC) of ARL patients was performed to analyze if Epstein–Barr VL could be related to response in these patients. Fifteen patients with ARL were included in this study with measurement of EBV VL at three different periods of time: at lymphoma diagnosis, upon completion of chemotherapy, and 3 months after. Two control groups composed by HIV-negative and HIV-positive patients were also evaluated for EBV VL comparison. In situ hybridization for EBER was performed on diagnostic samples of all ARL patients. Median EBV VL in PBMC and plasma had a significant decrease ($p = 0.022$ and $p = 0.003$, respectively) after ARL treatment. EBER was positive in 7 (46.7 %) cases. Median EBV VL in PBMC before lymphoma treatment in patients positive for EBER was significantly higher compared to EBER negative cases ($p = 0.041$). Reduction of EBV viral load during treatment of lymphoma could be predictive of response. EBER expression was associated to advanced stages of disease and worse immune status. Our study suggests that measurement of EBV VL during ARL treatment could be used as a marker for response, but further studies are needed to validate this association.

**Keywords** Aids-related lymphoma · HIV · EBV

## Short Communication

Human immunodeficiency virus (HIV) infection increases the risk for development of non-Hodgkin lymphoma by 100-fold compared to general population [1]. Most acquired immunodeficiency syndrome- related lymphomas

P. Y. Tanaka · J. Pereira
Faculdade de Medicina – Programa de Ciências Médicas, Universidade de São Paulo, Av. Dr. Arnaldo, 455, São Paulo, Brazil
e-mail: pyt@uol.com.br

K. Ohshima
Department of Pathology, School of Medicine, Kurume University, 67 Asahi-machi, Kurume-shi, Fukuoka-ken, Japan

M. Matsuoka
Institute for Virus Research, Kyoto University, 53 Asahi-machi, Kurume-shi, Fukuoka-ken, Japan

E. C. Sabino · S. C. Ferreira · A. S. Nishya
Laboratório de biologia molecular –Fundação pró-sangue, Av. Dr. Enéas de Carvalho Aguiar, 155, São Paulo, Brazil

R. de Oliveira Costa · J. Pereira
Instituto do Câncer do Estado de São Paulo, Av. Dr. Arnaldo, 251, São Paulo, Brazil

E. E. Calore · N. M. Perez
Pathology Section - Instituto de Infectologia Emílio Ribas, Av. Dr. Arnaldo, 165, São Paulo, Brazil

J. Pereira (✉)
Laboratório de Imunopatologia, Prédio de Ambulatórios do Hospital das Clinicas, Av. Dr. Enéas de Carvalho Aguiar, 255, 1°.andar, bloco 12 sala 61, Cep: 05403 – 001, São Paulo, Brazil
e-mail: julianapereira29@hotmail.com

(ARL) are diffuse large B cell lymphomas (DLBCL) and Burkitt lymphomas (BL). After introduction of highly active antiretroviral therapy (HAART) the incidence of ARL seems to be decreased mainly for primary central nervous system lymphoma (PCNSL). However, ARL remains the main cause of death related to AIDS in adults infected with HIV. Adverse prognostic factors for ARL included a CD4+ count less than 100 cells/μL, poor performance status, previous AIDS diagnosis and high risk in international prognostic index (IPI) [2]. The pathogenesis of ARL is associated to many factors including a continuous stimulation of B-cells by other viruses as Epstein–Barr virus (EBV) and human herpes virus type 8 with a poor immune status. EBV infection has been described in 40–90 % of ARL. The role of the EBV in pathogenesis and prognosis in ARL remains unclear [3]. EBV is not always found in the malignant cells but in cases of PCNSL and primary effusion lymphomas [4]. EBV viral load and EBV encoded small RNA (EBER) expression has been studied as prognostic factors in ARL with contradictory results [5, 6]. In order to analyze the impact of EBV viral load in serum and peripheral blood mononuclear cells (PBMC), EBER expression in ARL patients we performed a prospective and controlled study. Fifteen HIV-positive patients with DLBCL and BL according to the World Health Organization classification treated at Instituto de Infectologia Emilio Ribas and Hospital das Clínicas - FMUSP from January 2009 to March 2010 were studied. Patients were staged by Ann Arbor system and were treated with standard dose of CHOP (cyclophosphamide 750 mg/m$^2$ D1, doxorubicin 50 mg/m$^2$ D1, vincristine 1.4 mg/m$^2$ D1 and prednisone 60 mg/m$^2$ D1–D5) for 6–8 cycles. Central nervous system prophylaxis was performed for all cases using four intrathecal injection of cytarabine 50 mg plus dexamethasone 2 mg weekly in the first 4 weeks of treatment. In case of a cerebrospinal fluid involvement, intrathecal chemotherapy was administered twice-weekly, until total disappearance of the malignant cells. Granulocyte colony stimulating factor at dose of the 300 μg/day was indicated for all patients from day 5 of the chemotherapy cycle until the neutrophil counts exceeded 1.5 × 10$^9$/L. All patients received prophylaxis for *Pneumocystis carinii* and HAART was used for all patients. Zidovudine use was avoided due to hematological toxicity. The response to lymphoma treatment was assessed after cycles 4, 6 and 8 and was classified as complete response (CR), partial response, unconfirmed CR (CRu) or progressive disease (PD) according to International Workshop criteria [7]. Patients with PD or relapsed disease (RD) were treated with the salvage chemotherapy regimen ICE (ifosfamide, carboplatin, etoposide). Peripheral venous blood was harvested for EBV viral load measure at lymphoma diagnosis, after completion of chemotherapy, and 3 months afterwards. Two control groups composed by 26 HIV-positive patients without opportunistic infections and 30 HIV-negative individuals were also evaluated for EBV VL in PBMC and serum for comparison. Biopsy samples of lymphoma diagnosis were evaluated by situ hybridization for EBER analysis. This study was approved and informed consent was provided, according to the Brazilian Research Ethical Committee. Paraffin sections of tumor were processed for in situ hybridization using the EBER-PNA probe from DakoCytomation according to the manufacturer's instructions. Real-time polymerase chain reaction for EBV was performed using DNA extracted from 200 μL from serum and from PBMC that were obtained from whole blood before stored at −20 °C. For EBV viral load analysis the QIAamp DNA blood reactive from Qiagen was used. The detection value for EBV VL in serum was 68 copies/mL. For statistical analysis, the comparison between continuous variables in different groups was performed by Kruskal–Wallis test followed by Mann–Whitney's if results were significant. For discrete variables Fisher's exact test was done. Survival curves were estimated by Kaplan and Meier method. Wilcoxon's test was performed to compare EBV viral load in PBMC and serum in ARL patients at different times. To compare EBV viral load between serum and PBMC Spearman's correlation test was performed. For all analyzes significant results were considered for $p < 0.050$. Patient's clinical features are shown in Table 1, 13/15 (86.7 %) patients were male, with median age of 43 years (28–66 years). Risk factors for HIV infection included sexual contact was seen in 14/15 (93.3 %) and intravenous drug addict in 1/15 (6.7 %). DLBCL was found in 10/15 (66.7 %), BL in 4/15 (26.7 %) and PCNSL in 1/15 (6.7 %). Eleven (78.6 %) patients presented stage III or IV at diagnosis and the IPI score of high-intermediate and high-risk was observed in 7/15 (46.7 %) patients. Median CD4 T-cell count at diagnosis was 215 cells/μL (43–930) and 6/15 (40 %) patients showed HIV viral load above the cut-off point (50 copies/mL). Fourteen (93.3 %) patients were treated with CHOP and the patient with PCNSL received only radiotherapy. This patient acquired CR but died few months later. Nine (64.3 %) patients received full dose of CHOP and acquired CR. Five of nine patients (55 %) died later, two in relapsed disease. Other 2/15 patients died during chemotherapy and 2/15 presented PD and died, one of them after salvage chemotherapy. One patient abandoned treatment after the first cycle of chemotherapy and died later. All patients but one with relapsed disease died of sepsis. Four patients started HAART at the time of lymphoma diagnosis. Two patients received two nucleosides reverse transcriptase inhibitor (NRTI) plus one PI and two were treated with two NRTI plus 1 non-nucleoside reverse transcriptase inhibitor (NNRTI). Ten patients had been currently receiving HAART; four were using two NRTI plus

**Table 1** Characteristics of patients ($n = 15$)

| | |
|---|---|
| Age year, median (range) | 43.0 (28–66) |
| Sex, *n* (%) | |
| Female | 2 (13.3) |
| Male | 13 (86.7) |
| Risk factors HIV, *n* (%) | |
| Homosexual | 8 (53.3) |
| IVDU | 1 (6.7) |
| Heterosexual | 6 (40.0) |
| Prior aids, *n* (%) | |
| Yes | 11 (73.3) |
| No | 4 (26.7) |
| CD4 count cells/μL, *n* (%) | |
| <100 | 10 (66.7) |
| ≥100 | 5 (33.3) |
| Pathologic type, *n* (%) | |
| DLBCL | 10 (66.7) |
| BL | 4 (26.7) |
| PCNSL | 1 (6.7) |
| B symptoms, *n* (%) | |
| Present | 13 (86.7) |
| Absent | 2 (14.3) |
| Stage, *n* (%) | |
| I/II | 3 (21.4) |
| III/IV | 11 (78.6) |
| Extranodal sites, *n* (%) | |
| Yes | 12 (80.0) |
| No | 3 (20.0) |
| Number of extranodal sites, *n* (%) | |
| 0–1 | 9 (60.0) |
| ≥2 | 6 (40.0) |
| LDH level U/L, median(range) | 386.0 (161–10,308) |
| LDH level,n (%) | |
| ≤Normal | 7 (46.7) |
| >Normal | 8 (53.3) |

*IVDU* intravenous drug abuse, *AIDS* acquired immunodeficiency syndrome, *LDH* lactic dehydrogenase, *DLBCL* diffuse large B-cell lymphoma,*BL* Burkitt lymphoma, *PCNSL* primary central nervous system lymphoma

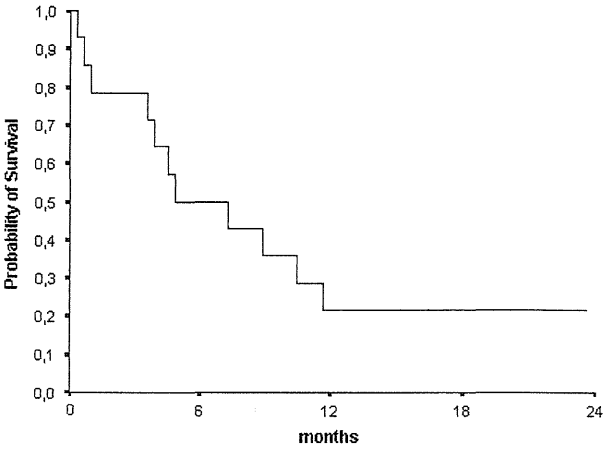


**Fig. 1** Probability of survival among patients with ARL

one PI, and six patients two NRTI plus one NNRTI. One patient did not use HAART, although prescribed before lymphoma diagnosis and the use of two NRTI plus one PI was initiated. There were no differences between the type of antiretroviral used and EBV viral load. EBV viral load in PBMCs and serum was performed for all patients at diagnosis, in 10/15 (66.6 %) patients after treatment and in four patients 3 months afterwards. Median EBV viral load before treatment was 1.3 copies/$10^6$ cells (0.1–147.2) in PBMC and were 40 copies/mL (0–24,900) in serum. During treatment the EBV viral load decrease to 0.05 copies/$10^6$ cells (0–10.9) in serum and was undetectable in PBMC. EBV viral load was significantly reduced after the last cycle of chemotherapy in comparison to diagnosis ($p = 0.022$ and $p = 0.003$, serum and PBMC, respectively). The EBV viral load remained not detectable or in low levels in PBMC and serum of patients with CR. Overall survival at 12 months of follow-up was 21.4 % (Fig. 1). No significant correlation was found between EBV viral load in PBMC or serum with CD4 T-cell counts and HIV viral load at diagnosis of lymphoma ($r = 0.166$ $p = 0.554$).In the control groups, EBV viral load in serum was not detectable (HIV-negative) and was lower in HIV-positive than in ARL patients ($p < 0.01$). The median of EBV viral load in PBMC in HIV-positive and HIV-negative control groups was 0.1 copy/$10^6$ PBMC (0–1.25) and undetectable, respectively. EBV viral load (PBMC) in ARL patients at diagnosis was higher than in HIV positive and HIV-negative control groups ($p = 0.002$ and $p < 0.001$, respectively). EBER was positive in 7/15 (46.7 %) of ARL in cases with more than 1 extranodal site ($p = 0.041$) and T CD4 counts less than 100 cells/μL ($p = 0.026$). Median EBV viral load in PBMC before treatment among patients with positive EBER expression was significantly higher compared to those with negative expression ($p = 0.041$). This study suggests that higher levels of EBV viral load could be associated with more aggressive lymphoma and poor immune status (measured by absolute counts of T-CD4 lymphocytes). There was a significant correlation between EBV load in PBMC and EBER expression in tumor cells. The real significance of EBV VL in the setting of the ARL still remains unclear. There aren't studies providing relevant evidence of EBV sequences inserted in tumor cells. Usually patients included have different status of HIV infection and do not account the adherence to antiretroviral therapy neither the type of immune reconstitution [8]. The type of EBV infection

latency in ARL patients has not been elucidated. EBV viral load does not seem to be predictive for ARL development, but some studies suggest it may be related to lymphoma treatment outcomes. Fan et al., detected EBV viral load in 74 % cases of 35 ARLs patients. EBV VL wasfound in the serum of all patients whose samples were positive for EBER ($n = 17$). In agreement with our study these authors demonstrated that EBV viral load decrease at completion of lymphoma therapy [9]. Bonnet et al., measured EBV viral load in whole blood of 14 ARL patients, 19 HIV non-AIDS patients and 20 HIV seronegative patients, with significant difference in patients with ARL compared to HIV-negative patients. Patients with ARL achieving CR had significant decrease in EBV VL [10].These data suggests that the decrease of EBV viral load during treatment of ARL could be related to response. EBER expression was present in 7/15 (46.5 %) of ARL patients and related to extranodal disease and CD4 T-cell count less than 100 cells/μL. These data indicates that EBER expression might be associated with more advanced disease and with severe immunodeficiency. Studies in patients with lymphoma without HIV infection have also correlated EBER expression with more advanced disease, similar to our results [11, 12]. In conclusion, our study suggests that measurement of EBV VL during ARL treatment could be a predictive factor for response, although further studies with a higher number of patients are needed to validate this association.

## References


1. Goedert JJ (2000) The epidemiology of acquired immunodeficiency syndrome malignancies. Semin Oncol 27(4):390–401
2. Tanaka PY, Pracchia LF, Bellesso M, Chamone DA, Calore EE, Pereira J (2010) A prognostic score for AIDS-related diffuse large B-cell lymphoma in Brazil. Ann Hematol 89(1):45–51
3. Young LS, Murray PG (2003) Epstein–Barr virus and oncogenesis: from latent genes to tumours. Oncogene 22(33):5108–5121
4. Bibas M, Antinori A (2009) EBV and HIV-related lymphoma. Mediterr J Hematol InfectDis 1(2):e2009032
5. van Baarle D, Hovenkamp E, Callan MF, Wolthers KC, Kostense S, Tan LC, Niesters HG, Osterhaus AD, McMichael AJ, van Oers MH, Miedema F (2001) Dysfunctional Epstein–Barr virus (EBV)-specific CD8(+) T lymphocytes and increased EBV load in HIV-1 infected individuals progressing to AIDS-related non-Hodgkin lymphoma. Blood 98(1):146–155
6. van Baarle D, Wolthers KC, Hovenkamp E, Niesters HG, Osterhaus AD, Miedema F, Van Oers MH (2002) Absolute level of Epstein–Barr virus DNA in human immunodeficiency virus type 1 infection is not predictive of AIDS-related non-Hodgkin lymphoma. J Infect Dis 186(3):405–409
7. Cheson BD, Horning SJ, Coiffier B, Shipp MA, Fisher RI, Connors JM, Lister TA, Vose J, Grillo-López A, Hagenbeek A, Cabanillas F, Klippensten D, Hiddemann W, Castellino R, Harris NL, Armitage JO, Carter W, Hoppe R, Canellos GP (1999) Reportof an international workshop to standardize response criteria for non-Hodgkin's lymphomas. NCI Sponsored International Working Group. J Clin Oncol 17(4):1244
8. O'Sullivan CE, Peng R, Cole KS, Montelaro RC, Sturgeon T, Jenson HB, Ling PD (2002) Epstein–Barr virus and human immunodeficiency virus serological responses and viral burdens in HIV-infected patients treated with HAART. J Med Virol 67(3):320–326
9. Fan H, Kim SC, Chima CO, Israel BF, Lawless KM, Eagan PA, Elmore S, Moore DT, Schichman SA, Swinnen LJ, Gulley ML (2005) Epstein–Barr viral load as a marker of lymphoma in AIDS patients. J Med Virol 75(1):59–69
10. Bonnet F, Jouvencel AC, Parrens M, Leon MJ, Cotto E, Garrigue I, Morlat P, Beylot J, Fleury H, Lafon ME (2006) A longitudinal and prospective study of Epstein–Barr virus load in AIDS-related non-Hodgkin lymphoma. J Clin Virol 36(4):258–263
11. Uner A, Akyurek N, Saglam A, Abdullazade S, Uzum N, Onder S, Barista I, Benekli M (2011) The presence of Epstein–Barr virus (EBV) in diffuse large B-cell lymphomas (DLBCLs) in Turkey: special emphasis on 'EBV-positive DLBCL of the elderly'. APMIS 119(4–5):309–316
12. Morales D, Beltran B, De Mendoza FH, Riva L, Yabar A, Quiñones P, Butera JN, Castillo J (2010) Epstein–Barr virus as a prognostic factor in de novo nodal diffuse large B-cell lymphoma. Leuk Lymphoma 51(1):66–72

Bioorganic & Medicinal Chemistry 23 (2015) 1447–1452

Contents lists available at ScienceDirect

Bioorganic & Medicinal Chemistry

journal homepage: www.elsevier.com/locate/bmc

# Identification of anti-HIV agents with a novel benzo[4,5]isothiazolo[2,3-*a*]pyrimidine scaffold

Shiho Okazaki [a], Tsukasa Mizuhara [a], Kazuya Shimura [b], Hiroto Murayama [b], Hiroaki Ohno [a], Shinya Oishi [a,*], Masao Matsuoka [b], Nobutaka Fujii [a,*]

[a] *Graduate School of Pharmaceutical Sciences, Kyoto University, Sakyo-ku, Kyoto 606-8501, Japan*
[b] *Institute for Virus Research, Kyoto University, Sakyo-ku, Kyoto 606-8507, Japan*

ARTICLE INFO

*Article history:*
Received 23 January 2015
Revised 6 February 2015
Accepted 10 February 2015
Available online 16 February 2015

*Keywords:*
Anti-HIV agent
Isothiazolopyrimidine
PD 404182
Pyrimidobenzothiazine

ABSTRACT

3,4-Dihydro-2*H*-benzo[4,5]isothiazolo[2,3-*a*]pyrimidine is a newly identified antiviral agent against human immunodeficiency virus type 1 (HIV-1) infection, derived from 3,4-dihydro-2*H*,6*H*-pyrimido-[1,2-*c*][1,3]benzothiazin-6-imine (PD 404182). The introduction of the hydrophobic 8-aryl substituent on the benzene substructure improved its anti-HIV activity, resulting in the identification of 6-fold more potent analogs. In addition, it was demonstrated that these isothiazolopyrimidine derivatives exert anti-HIV effects at an early stage of viral infection.



## 1. Introduction

A variety of anti-HIV drugs targeted to each stage of the infection have been developed for the treatment of human immunodeficiency virus (HIV) infection/acquired immunodeficiency syndrome (AIDS).[1] In particular, highly active antiretroviral therapy (HAART) by co-administration of nucleoside reverse transcriptase inhibitors (NRTIs), non-nucleoside reverse transcriptase inhibitors (NNRTIs), protease inhibitors (PIs) and integrase strand transfer inhibitors (INSTIs) is a standard treatment regimen for HIV-infected patients.[2] The HAART regimen strongly suppresses viral proliferation and has provided significant decline of morbidity and mortality,[3] but a complete cure or eradication of HIV has not yet been achieved. Long-term administration of multiple antiretroviral agents causes the emergence of drug-resistant HIV variants and drug-related adverse effects,[4,5] resulting in increased risk of virologic failure and/or limitation in the treatment strategy.[2] To overcome these problems, novel antiretroviral drugs with new mechanisms of action are now desired. Recently, a series of anti-HIV agents that inhibit an early stage of HIV infection are being explored, including the fusion inhibitor enfuvirtide,[6] a CC chemokine receptor type 5 (CCR5) antagonist (maraviroc),[7] CXC chemokine receptor type 4 (CXCR4) antagonists,[8,9] and CD4 mimics.[10]

Previously, we and others reported 3,4-dihydro-2*H*,6*H*-pyrimido[1,2-*c*][1,3]benzothiazin-6-imine (**1**, PD 404182)[11–14] as a new antiviral agent against human hepatitis C virus (HCV),[15,16] HIV,[16–20] simian immunodeficiency virus (SIV),[16] and herpes simplex virus (HSV) (Fig. 1).[20] A structure–activity relationship (SAR) study on compound **1** suggested that the 6-imino group and 7-sulfur atom were essential to interact with the potential target molecule(s), which was supported by a complete loss of its anti-HIV activity by substitution of these groups with other heteroatoms. Optimization of the benzene ring and the cyclic amidine moieties in the pyrimido[1,2-*c*][1,3]benzothiazin-6-imine scaffold demonstrated that the introduction of hydrophobic aryl moieties such as *m*-anisyl and 3,4-methylenedioxyphenyl groups into the 9-position improved the anti-HIV activity three-fold.[17,18] The antiviral profile of **1** indicated that the pyrimido[1,2-*c*][1,3]benzothiazin-6-imine derivatives inhibited early-stage HIV infection including virus attachment and membrane fusion to host cells as exemplified by DS 5000 (adsorption inhibitor)[21] and enfuvirtide (fusion inhibitor).[6] Although it was suggested that compound **1** exerts its virucidal effect against viral particles,[16,20] its antiviral mechanism of action has not yet been sufficiently detailed.

*Abbreviations:* CCR5, CC chemokine receptor type 5; CXCR4, CXC chemokine receptor type 4; MAGI, multinuclear activation of a galactosidase indicator; NNRTIs, non-nucleoside reverse transcriptase inhibitors; NRTIs, nucleoside reverse transcriptase inhibitors; PIs, protease inhibitors; INSTIs, integrase strand transfer inhibitors; PIDA, phenyliodine diacetate.

* Corresponding authors. Tel.: +81 75 753 4551; fax: +81 75 753 4570.
*E-mail addresses:* soishi@pharm.kyoto-u.ac.jp (S. Oishi), nfujii@pharm.kyoto-u.ac.jp (N. Fujii).

http://dx.doi.org/10.1016/j.bmc.2015.02.015
0968-0896/

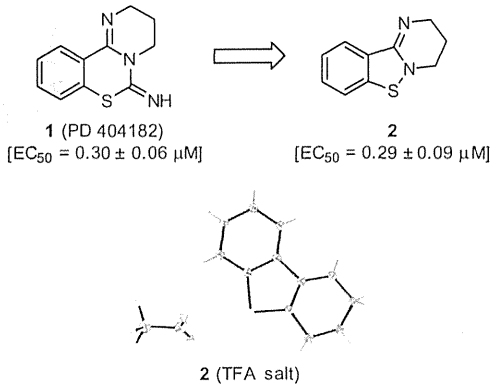


**Figure 1.** Structures of PD 404182 (**1**) and benzo[4,5]isothiazolo[2,3-*a*]pyrimidine (**2**).

During the course of our investigations of PD 404182 derivatives, 3,4-dihydro-2*H*-benzo[4,5]isothiazolo[2,3-*a*]pyrimidine **2** was found to exhibit potent anti-HIV activity ($EC_{50}$ = 0.29 μM) (Fig. 1). The structure of this unprecedented scaffold was verified by X-ray crystal analysis. Although there have been several reports that similar isothiazolidine and thiadiazole derivatives exhibited anti-HIV activities as zinc finger inhibitors for HIV-1 nucleocapsid protein 7 (NCp7),[22,23] this tetrahydropyrimidine-fused heterocyclic scaffold has not been explored as a potential anti-HIV agent candidate. In the current study, we investigated the synthesis of benzo[4,5]isothiazolo[2,3-*a*]pyrimidine derivatives and their structure–activity relationships as potent anti-HIV agents.

## 2. Results and discussion

### 2.1. Synthesis of benzo[4,5]isothiazolo[2,3-*a*]pyrimidine derivatives

Our investigation began with the synthesis of benzo[4,5]isothiazolo[2,3-*a*]pyrimidine scaffold **9** having a characteristic S–N covalent bond, formed by oxidation of 2-(tetrahydropyrimidin-2-yl)-thiophenol derivative **8** (Scheme 1). Previously we reported the synthesis of PD 404182 derivative **6** with the pyrimido[1,2-*c*]-[1,3]benzothiazin-6-imine core.[17–19,24] Briefly, the oxidative amidination[25] of various benzaldehydes **3** gave the corresponding 2-phenyltetrahydropyrimidine derivative **4**. $S_NAr$-type C–*S* bond formation on **4** with *tert*-butyl isothiocyanate afforded *N*-(*tert*-butyl)-protected thiazinimine **5**, which was subjected to deprotection of the *tert*-butyl group with trifluoroacetic acid (TFA) to provide PD 404182 derivative **6**. The subsequent TFA-mediated ethanolysis of the imino group in **6c–i,k,l,n** generated the thiophenol precursor **8**. Without isolation of the thiophenol **8**, the desired benzo[4,5]isothiazolo[2,3-*a*]pyrimidines **9c–i,k,l,n** were obtained after linking the thiol group and cyclic amidine NH group by phenyliodine diacetate (PIDA)[26]-mediated oxidation. Alternatively, pyrimido[1,2-*c*][1,3]benzothiazin-6-thione derivatives **7j,m** were synthesized by addition of carbon disulfide to derivatives **4j,m** followed by $S_NAr$-type C–S bond formation.[24,27] Alkaline hydrolysis of the thiocarbonyl group of **7j,m** followed by PIDA-mediated oxidation gave the compounds **9j,m**. The benzo[4,5]isothiazolo-[2,3-*a*]pyrimidine derivatives **9c–n** were derivatized from benzothiazin-6-imine **6** and the precursor **7**,[24] which were employed for our previous structure–activity relationship studies of PD 404182 derivatives.[17,18]

A series of 8-aryl benzo[4,5]isothiazolo[2,3-*a*]pyrimidine derivatives **9a,b,o–z** were also prepared by the identical protocol (Scheme 2).[18] A Suzuki–Miyaura cross-coupling reaction of

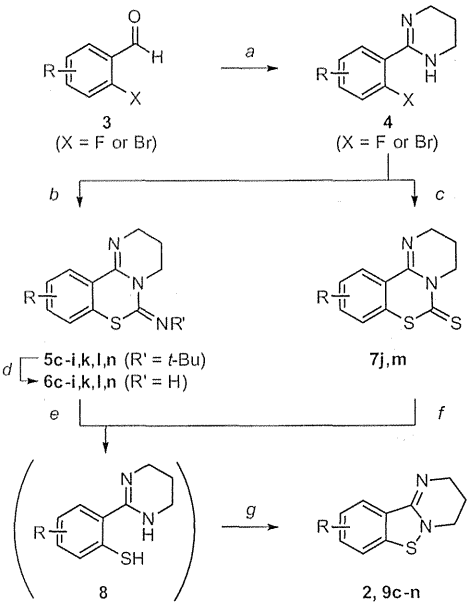


**Scheme 1.** Synthesis of 7-, 8- and 9-substituted benzo[4,5]isothiazolo[2,3-*a*]pyrimidine derivatives. Reagents and conditions: (a) 1,3-propanediamine, $I_2$, $K_2CO_3$, *t*-BuOH, 70 °C; (b) NaH or *t*-BuOK, *t*-BuNCS, DMF or DMAc, −20–80 °C; (c) NaH, $CS_2$, DMF, rt–80 °C; (d) TFA, MS4Å, $CHCl_3$, reflux; (e) TFA, $CHCl_3$/EtOH, rt; (f) NaOH, MeOH/$H_2O$, reflux; (g) PIDA, $CHCl_3$/EtOH or $CHCl_3$, rt.

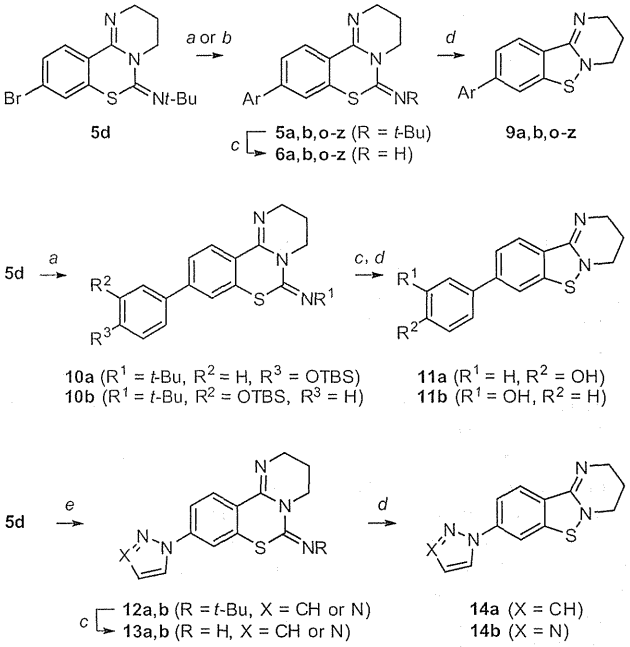


**Scheme 2.** Synthesis of 8-aryl benzo[4,5]isothiazolo[2,3-*a*]pyrimidines. Reagents and conditions: (a) Ar-B(OH)$_2$, Pd(PPh$_3$)$_4$, Pd(dppf)Cl$_2$·CH$_2$Cl$_2$, $K_2CO_3$, toluene/EtOH/$H_2O$, reflux; (b) 2-pyridinyltriolborate lithium salt, Pd(OAc)$_2$, CuI, PPh$_3$, DMF, 80 °C; (c) TFA, MS4Å, $CHCl_3$, reflux; (d) TFA, $CHCl_3$/EtOH or EtOH, rt, then Et$_3$N, PIDA, $CHCl_3$/EtOH or EtOH, rt; (e) pyrazole or triazole, CuCl, $K_2CO_3$, acetylacetone, NMP, 130 °C.

bromide **5d** with aryl boronic acid provided compounds **5a,b,o–z**. For the synthesis of 8-(pyridin-2-yl) derivative **9x**, 2-pyridinyltriolborate lithium salt was employed. Subsequent deprotection of the *tert*-butyl group of compound **5** gave the corresponding thiazinimine **6a,b,o–z**. After TFA-mediated alcoholysis of compound

**6**, PIDA-mediated S–N bond formation afforded the desired 8-aryl benzo[4,5]isothiazolo[2,3-*a*]pyrimidines **9a**,**b**,**o**–**z**. For the preparation of *p*-hydroxyphenyl and *m*-hydroxyphenyl compounds **11a**,**b**, the TBS and *tert*-butyl protecting groups in the precursors **10a**,**b** were consecutively removed. Ullmann coupling of bromide **5d** with azoles followed by subsequent manipulations afforded pyrazole and triazole derivatives **14a**,**b**.

### 2.2. Structure–activity relationship study of the anti-HIV activity of benzo[4,5]isothiazolo[2,3-*a*]pyrimidine derivatives

Initially, we investigated the modifications of the benzo-[4,5]isothiazolo[2,3-*a*]pyrimidine derivatives at the 7-, 8- and 9-positions (Table 1). The anti-HIV activity of a series of compounds was evaluated by the NCK assay,[28] in which the inhibition of virus attachment and membrane fusion to host cells during early-stage HIV infection is evaluated. The 8-phenyl modification (**9a**) maintained the potency of the lead compound **2** ($EC_{50}$ = 0.30 μM), while the *m*-anisyl (**9b**) and bromo (**9d**) derivative exhibited two to three times greater anti-HIV activity ($EC_{50}$ (**9b**) = 0.10 μM, $EC_{50}$ (**9d**) = 0.22 μM). In contrast, the methoxy (**9c**), trifluoromethyl (**9e**) and nitro (**9f**) groups slightly decreased the anti-HIV activity, and the 8-acetamide group in **9g** remarkably attenuated the activity. Modifications at the 9-position of benzo[4,5]isothiazolo[2,3-*a*]-pyrimidine were also unfavorable for anti-HIV activity. 9-Phenyl (**9i**), methyl (**9j**), methoxy (**9k**), bromo (**9l**) and trifluoromethyl (**9m**)-modified derivatives showed two- to seven-fold less anti-HIV activity compared with compound **2**. The 7,8-fused benzene (**9h**) (naphtho[2′,1′:4,5]isothiazolo[2,3-*a*]pyrimidine) and 7-bromo (**9n**) substituent exhibited cytotoxicity at 10 μM with a loss of anti-HIV activity.

On the basis of the initial structure–activity relationships of the benzo[4,5]isothiazolo[2,3-*a*]pyrimidine derivatives, further modifications on the 8-aryl substituent were carried out (Table 2). First, we modified the *para*- and *meta*-positions of the 8-phenyl group in compound **9a**. The methoxy (**9o** and **9b**), methoxycarbonyl (**9p** and **9r**) and nitro (**9q** and **9s**) groups improved the anti-HIV activity ($EC_{50}$ = 0.05–0.16 μM), which was approximately two- to six-fold greater compared with compound **2**. Because the effects by introduction of electron-withdrawing and electron-donating substituents on the aromatic ring were similar, the electron density of the 8-phenyl group is unlikely to be the primary factor for the interaction with the target molecule(s). *Para*- and *meta*-hydroxy groups (**11a** and **11b**) reduced the anti-HIV activity ($EC_{50}$ = 1.28 and 1.47 μM, respectively). The substitution of the 8-phenyl group with a variety of hetero- and carbocyclic substructures was also investigated. The hydrophobic 3,4-methylenedioxyphenyl (**9t**), 2-naphthyl (**9u**), furan-2-yl (**9v**) and thiophen-3-yl (**9w**) groups increased the anti-HIV activity. In contrast, substitution with basic heterocycles such as pyridine (**9x**–**z**), pyrazole (**14a**) and triazole (**14b**) resulted in a slight decrease of the anti-HIV activity compared with compound **9a**, suggesting that nitrogen heterocycles are not favorable at this position. These results indicated that favorable hydrophobic interaction(s) of the 8-aryl groups with the potential target molecule(s) could play important roles for determining the anti-HIV activity. Cytotoxic effects were not observed at 10 μM except for compound **9o**.

### 2.3. Mechanistic studies of anti-HIV isothiazolopyrimidine derivatives

We executed a time of drug addition study to estimate the mechanism of action of the isothiazolopyrimidine derivatives (Fig. 2). In our previous studies, we determined that PD 404182 (**1**) and its derivatives inhibited an early stage of HIV infection.[17,18] In this study, compound **2** and potent derivatives **9r** and **9v** were evaluated for their anti-HIV activity profiles compared with anti-HIV agents including DS 5000 (adsorption inhibitor),[21] enfuvirtide (fusion inhibitor),[6] AZT (NRTI),[29] nevirapine (NNRTI),[30] and raltegravir (integrase inhibitor).[31] Isothiazolopyrimidine derivatives **2**, **9r**, and **9v** had similar inhibitory profiles to that of DS 5000 and compound **1**, which prevent an early stage of viral infection including the attachment and entry into the target cells. It should also be noted that both compounds **1** and **2** showed a broad spectrum of antiviral activity against RNA viruses and DNA viruses (data not shown). These results may suggest that these two series of compounds may have an identical or similar target molecule(s) or mechanism of action for the antiviral activities. Although a possible common viral target molecule(s) has not yet been identified,[32] these derivatives could positively regulate the defense mechanism(s) of the host cells.

**Table 1**
Structure–activity relationships of benzo[4,5]isothiazolo[2,3-*a*]pyrimidine derivatives

| Compd | | $EC_{50}$[a] (μM) | Compd | | $EC_{50}$[a] (μM) |
|---|---|---|---|---|---|
| | 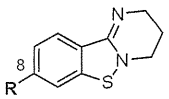 | | | 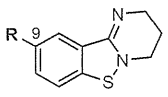 | |
| **2** | R = H | 0.29 ± 0.09 | | | |
| **9a** | R = Ph | 0.30 ± 0.10 | **9i** | R = Ph | 0.56 ± 0.13 |
| **9b** | R = *m*-anisyl | 0.10 ± 0.03 | **9j** | R = Me | 0.85 ± 0.10 |
| **9c** | R = OMe | 0.58 ± 0.10 | **9k** | R = OMe | 2.11 ± 0.48 |
| **9d** | R = Br | 0.22 ± 0.07 | **9l** | R = Br | 1.01 ± 0.22 |
| **9e** | R = $CF_3$ | 1.28 ± 0.04 | **9m** | R = $CF_3$ | 1.78 ± 0.24 |
| **9f** | R = $NO_2$ | 1.79 ± 0.44 | | | |
| **9g** | R = NHAc | >10 | | | |
| **9h** | 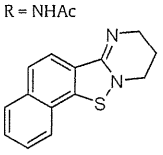 | >1.0[b,c] | **9n** | 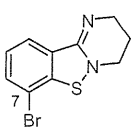 | >10[c] |

[a] $EC_{50}$ values represent the concentration of the compound required to inhibit the HIV-1 infection by 50%. The data were obtained from three independent experiments by the NCK assay.
[b] The compound inhibited the HIV-1 infection by 40% at 1.0 μM.
[c] Cytotoxicity was observed at 10 μM.

**Table 2**
Structure–activity relationship of 8-aryl benzo[4,5]isothiazolo[2,3-*a*]pyrimidines

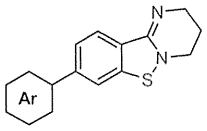


| Compd | | | $EC_{50}$[a] (μM) | Compd | | $EC_{50}$[a] (μM) |
|---|---|---|---|---|---|---|
| **9a** |  | | 0.30 ± 0.10 | | | |
| **9o** | 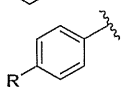 | R = OMe | 0.09 ± 0.03[b] | **9v** |  | 0.05 ± 0.02 |
| **9p** | | R = $CO_2Me$ | 0.16 ± 0.02 | | | |
| **9q** | | R = NO | 0.08 ± 0.01 | | | |
| **11a** | | R = $OH_2$ | 1.28 ± 0.26 | **9w** |  | 0.08 ± 0.01 |
| **9b** | 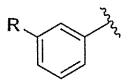 | R = OMe | 0.10 ± 0.03 | **9x** |  | 0.34 ± 0.11 |
| **9r** | | R = $CO_2Me$ | 0.05 ± 0.01 | | | |
| **9s** | | R = $NO_2$ | 0.12 ± 0.04 | | | |
| **11b** | | R = OH | 1.47 ± 0.24 | **9y** |  | 0.56 ± 0.03 |
| **9t** | 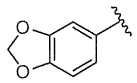 | | 0.16 ± 0.02 | **9z** |  | 0.56 ± 0.17 |
| | | | | **14a** |  | 0.41 ± 0.07 |
| **9u** | 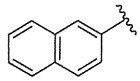 | | 0.12 ± 0.03 | **14b** |  | 0.42 ± 0.10 |

[a] $EC_{50}$ values represent the concentration of the compound required to inhibit the HIV-1 infection by 50%. The data were obtained from three independent experiments by the NCK assay.
[b] Cytotoxicity was observed at 10 μM.

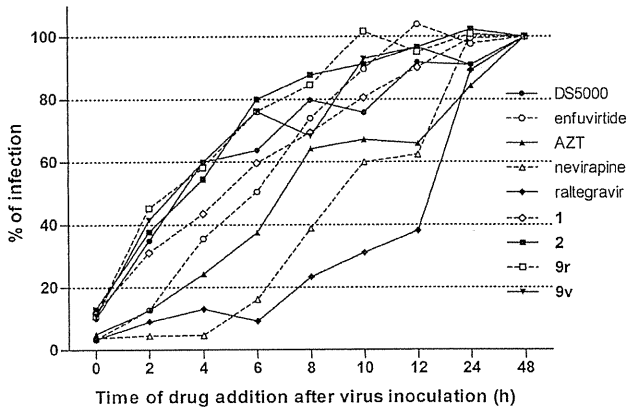


**Figure 2.** Time of drug addition profiles for HIV-1 infection.

## 3. Conclusions

In this study, we identified a novel class of small-molecule anti-HIV agents with the benzo[4,5]isothiazolo[2,3-*a*]pyrimidine scaffold. A structure–activity relationship study of the lead compound **2** demonstrated that a hydrophobic aryl substituent at the 8-position of the scaffold was responsible for the potent anti-HIV activity. Although the improvement of the anti-HIV activity from **2** was not satisfactory, further SAR studies would provide promising candidates with higher potency and favorable antiviral profiles. The similar antiviral profiles between compounds **1** and **2** suggested that these could possibly binds with the common potential target molecule(s) in host cells. The identification of the target molecule(s) and further optimization of potent derivatives should facilitate the development of novel antiviral agents.

## 4. Experimental section

### 4.1. Synthesis

#### 4.1.1. General synthesis

$^1H$ NMR spectra were recorded using a JEOL AL-400 or a JEOL ECA-500 spectrometer. Chemical shifts are reported in $\delta$ (ppm) relative to $Me_4Si$ as an internal standard. $^{13}C$ NMR spectra were referenced to the residual solvent signal. Exact mass (HRMS) spectra were recorded on a JMS-HX/HX 110A mass spectrometer or Shimadzu LC-ESI-IT-TOF-MS equipment. For flash chromatography, Wakogel C-300E (Wako) was employed. For analytical HPLC, a Cosmosil 5C18-ARII column (4.6 × 250 mm, Nacalai Tesque, Inc.) was employed with a linear gradient of $CH_3CN$ containing 0.1% (v/v) TFA aq. at a flow rate of 1 mL/min, and eluting products were detected by UV at 254 nm. Preparative HPLC was performed using a Cosmosil 5C18-ARII preparative column (20 × 250 mm, Nacalai Tesque, Inc.) with a linear gradient of $CH_3CN$ containing 0.1% (v/v) TFA aq. at a flow rate of 8 mL/min. The purity of the compounds was determined as no less than 95% by combustion analysis or HPLC analysis.

#### 4.1.2. General procedure for the synthesis of benzo[4,5]isothiazolo[2,3-*a*]pyrimidine from pyrimido[1,2-*c*]-[1,3]benzothiazin-6-imine: synthesis of 3,4-dihydro-2*H*-benzo-[4,5]isothiazolo[2,3-*a*]pyrimidine (2)

TFA (171 μL, 2.30 mmol) was added to a suspension of PD 404182 (**1**) (50.0 mg, 0.230 mmol) in $CHCl_3$ (2.30 mL) and EtOH (3.43 mL) dropwise. After being stirred at room temperature for 1 h, the mixture was quenched with $Et_3N$ (321 μL, 2.30 mmol), and PIDA (72.6 mg, 0.226 mmol) was added. After being stirred for 30 min at room temperature, the mixture was concentrated. Crude product was purified by HPLC to give the title compound **2** as colorless crystals (48.5 mg, 71%, TFA salt); mp 200–202 °C (from $Et_2O$–MeOH); IR (neat) $cm^{-1}$: 3117–3056 (OH), 1662 (C=O), 1630 (C=N); $^1H$ NMR (500 MHz, $CD_3OD$): $\delta$ 2.30–2.35 (m, 2H, $CH_2$), 3.67 (t, $J$ = 5.4 Hz, 2H, $CH_2$), 4.16 (t, $J$ = 5.7 Hz, 2H, $CH_2$), 7.63–7.66 (m, 1H, Ar), 7.84–7.87 (m, 1H, Ar), 8.04 (d, $J$ = 8.6 Hz, 1H, Ar), 8.17 (d, $J$ = 8.0 Hz, 1H, Ar); $^{13}C$ NMR (125 MHz, $CD_3OD$): $\delta$ 20.7, 39.0, 46.3, 118.3 (q, $J$ = 293.9 Hz), 122.5, 123.0, 125.1, 128.2, 134.7, 143.5, 156.0, 163.0 (q, $J$ = 34.8 Hz); Anal. Calcd for $C_{12}H_{11}F_3N_2O_2S$: C, 47.37; H, 3.64; N, 9.21. Found: C, 47.32; H, 3.80; N, 9.29.

#### 4.1.3. 9-Methyl-3,4-dihydro-2*H*-benzo[4,5]isothiazolo[2,3-*a*]-pyrimidine (9j)

10-Methyl-3,4-dihydro-2*H*,6*H*-pyrimido[1,2-*c*][1,3]benzothiazine-6-thione (**7j**) (60.0 mg, 0.242 mmol) was suspended in 0.1 N NaOH in MeOH–$H_2O$ (9:1, 4.83 mL). After being stirred under reflux for 12 h, the mixture was quenched with 1 N HCl until pH was adjusted to 7. The whole was extracted with $CHCl_3$–MeOH (95:5), and dried over $MgSO_4$. After concentration, the residue in $CHCl_3$ (6.04 mL) was allowed to react with PIDA (76.3 mg, 0.237 mmol). After being stirred for 30 min at room temperature, the mixture was concentrated. Purification by HPLC gave the title compound **9j** as colorless solid (4.5 mg, 6%, TFA salt); IR (neat) $cm^{-1}$: 3265–3141 (OH), 1669 (C=O), 1630 (C=N); $^1H$ NMR (500 MHz, $CD_3OD$): $\delta$ 2.29–2.34 (m, 2H, $CH_2$), 2.53 (s, 3H, $CH_3$), 3.66 (t, $J$ = 5.7 Hz, 2H, $CH_2$), 4.14 (t, $J$ = 5.7 Hz, 2H, $CH_2$), 7.71 (dd, $J$ = 8.3, 1.4 Hz, 1H, Ar), 7.91 (d, $J$ = 8.6 Hz, 1H, Ar), 7.96 (d, $J$ = 1.7 Hz, 1H, Ar); $^{13}C$ NMR (125 MHz, $CD_3OD$): $\delta$ 20.7, 21.1, 38.9, 46.3, 118.6 (q, $J$ = 255.5 Hz), 122.1, 123.0, 124.6, 136.2, 139.0, 140.6, 155.7, 162.7 (q, $J$ = 33.6 Hz); HRMS (FAB): *m/z* calcd for $C_{11}H_{13}N_2S$ $[M+H]^+$ 205.0799; found: 205.0795.

#### 4.1.4. 8-(4-Hydroxyphenyl)-3,4-dihydro-2*H*-benzo[4,5]isothiazolo[2,3-*a*]pyrimidine (11a)

TFA (2.35 mL) was added to a mixture of *N*-(*tert*-butyl)-9-[4-(*tert*-butyldimethylsilyloxy)phenyl]-3,4-dihydro-2*H*,6*H*-pyrimido-[1,2-*c*][1,3]benzothiazin-6-imine (**10a**) (112.6 mg, 0.235 mmol) in a few drops of $CHCl_3$ and MS4Å (528 mg, powder, activated by heating with Bunsen burner). After being stirred under reflux for 4 h, the mixture was added dropwise $Et_3N$ at 0 °C to adjust pH to 8–9. The whole was extracted with EtOAc. The extract was washed with sat. $NaHCO_3$, brine, and dried over $MgSO_4$. Concentration gave the crude imine as pale yellow solid (73.9 mg). By use of a procedure similar to that described for the preparation of the compound **2** from **1**, a part of the residue (20.0 mg) was converted to the title compound **11a** as colorless solid (11.0 mg, 44% in 2 steps, TFA salt); IR (neat) $cm^{-1}$: 3237–3066 (OH), 1684 (C=O), 1632 (C=N); $^1H$ NMR (500 MHz, $CD_3OD$): $\delta$ 2.31–2.35 (m, 2H, $CH_2$), 3.67 (t, $J$ = 5.7 Hz, 2H, $CH_2$), 4.15 (t, $J$ = 6.0 Hz, 2H, $CH_2$), 6.91–6.94 (m, 2H, Ar), 7.60–7.63 (m, 2H, Ar), 7.86 (dd, $J$ = 8.6, 1.1 Hz, 1H, Ar), 8.15 (d, $J$ = 8.6 Hz, 1H, Ar), 8.19 (d, $J$ = 1.7 Hz, 1H, Ar); $^{13}C$ NMR (125 MHz, $CD_3OD$): $\delta$ 20.7, 39.0, 46.2, 117.1 (2C), 118.2 (q, $J$ = 238.7 Hz), 119.0, 120.8, 125.3, 126.7, 129.8 (2C), 130.8, 144.3, 147.7, 155.7, 160.0, 162.9 (q, $J$ = 34.8 Hz); HRMS (ESI): *m/z* calcd for $C_{16}H_{15}N_2OS$ $[M+H]^+$ 283.0905; found: 283.0908.

### 4.2. Anti-HIV activity

The anti-HIV activity of a series of compounds against HIV-$1_{IIIB}$ was determined by the NCK assay.[28] The target cells (NCK45-β-Gal; $10^4$ cells/well) were plated in 96-well flat microtiter culture plates. On the following day, the cells were inoculated with HIV-1 (60 NCK U/well, giving 60 blue cells after 48 h of incubation) and cultured in the presence of various concentrations of the test compounds in fresh medium. Forty-eight hours after viral exposure, all the blue cells stained with X-Gal (5-bromo-4-chloro-3-indolyl-β-D-galactopyranoside) were counted in each well. The activity of test compounds was determined as the concentration that blocked HIV-1 infection by 50% (50% effective concentration [$EC_{50}$]). $EC_{50}$ was determined by using the following formula:

$$EC_{50} = 10^{\wedge}[\log(A/B) \times (50 - C)/(D - C) + \log(B)],$$

where

A: of the two points on the graph that bracket 50% inhibition, the higher concentration of the test compound,
B: of the two points on the graph that bracket 50% inhibition, the lower concentration of the test compound,
C: inhibitory activity (%) at the concentration B,
D: inhibitory activity (%) at the concentration A.


## Acknowledgments

This work was supported by Grants-in-Aid for Scientific Research from JSPS, Japan; Platform for Drug Discovery, Informatics, and Structural Life Science from MEXT, Japan; a Grant-in-Aid for Research on HIV/AIDS from the Ministry of Health and Welfare of Japan. T.M. is grateful for JSPS Research Fellowships for Young Scientists.


## Supplementary data

Supplementary data associated with this article can be found, in the online version, at http://dx.doi.org/10.1016/j.bmc.2015.02.015.

## References and notes


1. For a recent review, see: Barré-Sinoussi, F.; Ross, A. L.; Delfraissy, J. *Nat. Rev. Microbiol.* **2013**, *11*, 877.
2. Günthard, H. F.; Aberg, J. A.; Eron, J. J.; Hoy, J. F.; Telenti, A.; Benson, C. A.; Burger, D. M.; Cahn, P.; Gallant, J. E.; Glesby, M. J.; Reiss, P.; Saag, M. S.; Thomas, D. L.; Jacobsen, D. M.; Volberding, P. A. *J. Am. Med. Assoc.* **2014**, *312*, 410.
3. Wang, C.; Vlahov, D.; Galai, N.; Bareta, J.; Strathdee, S. A.; Nelson, K. E.; Sterling, T. R. *J. Infect. Dis.* **2004**, *190*, 1046.
4. Siliciano, J. D.; Siliciano, R. F. *Curr. Opin. Virol.* **2013**, *3*, 487.
5. Carr, A. *Nat. Rev. Drug. Disc.* **2003**, *2*, 624.
6. Matthews, T.; Salgo, M.; Greenberg, M.; Chung, J.; DeMasi, R.; Bolognesi, D. *Nat. Rev. Drug. Disc.* **2004**, *3*, 215.
7. Dorr, P.; Westby, M.; Dobbs, S.; Griffin, P.; Irvine, B.; Macartney, M.; Mori, J.; Rickett, G.; Smith-Burchnell, C.; Napier, C.; Webster, R.; Armour, D.; Price, D.; Stammen, B.; Wood, A.; Perros, M. *Antimicrob. Agents Chemother.* **2005**, *49*, 4721.
8. For a recent review, see: Choi, W. T.; Duggineni, S.; Xu, Y.; Huang, Z.; An, J. *J. Med. Chem.* **2012**, *55*, 977.
9. For our recent study, see: Kobayashi, K.; Oishi, S.; Hayashi, R.; Tomita, K.; Kubo, T.; Tanahara, N.; Ohno, H.; Yoshikawa, Y.; Furuya, T.; Hoshino, M.; Fujii, N. *J. Med. Chem.* **2012**, *55*, 2746, and references therein.
10. Zhao, Q.; Ma, L.; Jiang, S.; Lu, H.; Liu, S.; He, Y.; Strick, N.; Neamati, N.; Debnath, A. K. *Virology* **2005**, *339*, 213.
11. PD 404182 (**1**) was previously reported to be an enzyme inhibitor against 3-deoxy-D-*manno*-octulosonic acid 8-phosphate synthase[12] and phosphopantetheinyl transferase.[13] In addition, it was recently reported that PD 404182 (**1**) inhibits human dimethylarginine dimethylaminohydrolase isoform 1 (DDAH).[14]
12. Birck, M. R.; Holler, T. P.; Woodard, R. W. *J. Am. Chem. Soc.* **2000**, *122*, 9334.
13. Duckworth, B. P.; Aldrich, C. C. *Anal. Biochem.* **2010**, *403*, 13.
14. Ghebremariam, Y. T.; Erlanson, D. A.; Cooke, J. P. *J. Pharmacol. Exp. Ther.* **2014**, *348*, 69.

15. Chockalingam, K.; Simeon, R. L.; Rice, C. M.; Chen, Z. *Proc. Natl. Acad. Sci. U.S.A.* **2010**, *107*, 3764.
16. Chamoun, A. M.; Chockalingam, K.; Bobardt, M.; Simeon, R.; Chang, J.; Gallay, P.; Chen, Z. *Antimicrob. Agents Chemother.* **2012**, *56*, 672.
17. Mizuhara, T.; Oishi, S.; Ohno, H.; Shimura, K.; Matsuoka, M.; Fujii, N. *Org. Biomol. Chem.* **2012**, *10*, 6792.
18. Mizuhara, T.; Oishi, S.; Ohno, H.; Shimura, K.; Matsuoka, M.; Fujii, N. *Bioorg. Med. Chem.* **2012**, *20*, 6434.
19. Mizuhara, T.; Oishi, S.; Ohno, H.; Shimura, K.; Matsuoka, M.; Fujii, N. *Bioorg. Med. Chem.* **2013**, *21*, 2079.
20. Chamoun-Emanuelli, A. M.; Bobardt, M.; Moncla, B.; Mankowski, M. K.; Ptak, R. G.; Gallay, P.; Chen, Z. *Antimicrob. Agents Chemother.* **2014**, *58*, 687.
21. Baba, M.; Schols, D.; Pauwels, R.; Nakashima, H.; De Clercq, E. *J. Acquir. Immune Defic. Syndr.* **1990**, *3*, 493.
22. Loo, J. A.; Holler, T. P.; Sanchez, J.; Gogliotti, R.; Maloney, L.; Reily, M. D. *J. Med. Chem.* **1996**, *39*, 4313.
23. Vercruysse, T.; Basta, B.; Dehaen, W.; Humbert, N.; Balzarini, J.; Debaene, F.; Sanglier-Cianférani, S.; Pannecouque, C.; Mély, Y.; Daelemans, D. *Retrovirology* **2012**, *9*, 95.
24. Mizuhara, T.; Oishi, S.; Fujii, N.; Ohno, H. *J. Org. Chem.* **2010**, *75*, 265.
25. Ishihara, M.; Togo, H. *Tetrahedron* **2007**, *63*, 1474.
26. Among several reagents assessed for the oxidative cyclization including *m*CPBA, NBS, and iodosylbenzene, PIDA provided the most efficient S–N bond formation.
27. The synthetic process via 1,3-thiazine-2-thione intermediates **7j,m** was chosen for compounds **9j,m** because of the substrate availability.
28. Kajiwara, K.; Kodama, E.; Sakagami, Y.; Naito, T.; Matsuoka, M. *J. Clin. Microbiol.* **2008**, *46*, 792.
29. Fischl, M. A.; Richman, D. D.; Grieco, M. H.; Gottlieb, M. S.; Volberding, P. A.; Laskin, O. L.; Leedom, J. M.; Groopman, J. E.; Mildvan, D.; Schooley, R. T.; Jackson, G. G.; Durack, D. T.; King, D. N. *Engl. J. Med.* **1987**, *317*, 185.
30. Skoog, M. T.; Hargrave, K. D.; Miglietta, J. J.; Kopp, E. B.; Merluzzi, V. J. *Med. Res. Rev.* **1992**, *12*, 27.
31. Summa, V.; Petrocchi, A.; Bonelli, F.; Crescenzi, B.; Donghi, M.; Ferrara, M.; Fiore, F.; Gardelli, C.; Gonzalez Paz, O.; Hazuda, D. J.; Jones, P.; Kinzel, O.; Laufer, R.; Monteagudo, E.; Muraglia, E.; Nizi, E.; Orvieto, F.; Pace, P.; Pescatore, G.; Scarpelli, R.; Stillmock, K.; Witmer, M. V.; Rowley, M. *J. Med. Chem.* **2008**, *51*, 5843.
32. Of note, it was reported that PD 404182 showed the antiviral activities by virucidal effect via the physical disruption of virions, see Refs. 16,20.

Organic & Biomolecular Chemistry

PAPER

View Article Online
View Journal



Cite this: DOI: 10.1039/c5ob00301f

# Investigations of possible prodrug structures for 2-(2-mercaptophenyl)tetrahydropyrimidines: reductive conversion from anti-HIV agents with pyrimidobenzothiazine and isothiazolopyrimidine scaffolds†

Shiho Okazaki,[a] Shinya Oishi,*[a] Tsukasa Mizuhara,[a] Kazuya Shimura,[b] Hiroto Murayama,[b] Hiroaki Ohno,[a] Masao Matsuoka[b] and Nobutaka Fujii*[a]

Received 12th February 2015,
Accepted 9th March 2015

DOI: 10.1039/c5ob00301f

www.rsc.org/obc

3,4-Dihydro-2*H*,6*H*-pyrimido[1,2-*c*][1,3]benzothiazin-6-imine (PD 404182) and 3,4-dihydro-2*H*-benzo-[4,5]isothiazolo[2,3-*a*]pyrimidine are the heterocyclic antiretroviral agents against human immunodeficiency virus type 1 (HIV-1) infection. On the basis of similar structure–activity relationships of anti-HIV activities toward the early-stage of viral infection between these unique scaffolds, the transformations under the bioassay conditions were investigated. The distinctive S–N bond in the isothiazolopyrimidine scaffold was immediately cleaved under reductive conditions in the presence of GSH to generate a thiophenol derivative. A similar rapid conversion of PD 404182 into the same thiophenol derivative was observed, suggesting that pyrimidobenzothiazine and isothiazolopyrimidine scaffolds may work as prodrug forms of the common bioactive thiophenol derivatives.

## Introduction

PD 404182 (**1a**, 3,4-dihydro-2*H*,6*H*-pyrimido[1,2-*c*][1,3]benzothiazin-6-imine)[1–4] is an antiviral agent against human hepatitis C virus (HCV),[5,6] HIV,[6–10] simian immunodeficiency virus (SIV),[6] and herpes simplex virus (HSV) (Fig. 1).[10] 3,4-Dihydro-2*H*-benzo[4,5]isothiazolo[2,3-*a*]pyrimidine **2a** with a unique heterocyclic scaffold also exhibits potent anti-HIV activity ($EC_{50}$ = 0.29 ± 0.09 μM) (Fig. 1).[11] In our recent studies, we revealed that modification of the 9-position of PD 404182 derivatives with hydrophobic aryl groups improved the anti-HIV activity.[7–9] For example, the introduction of an aryl (**1b**, **1c** and **1f**) or bromo (**1d**) substituent at the 9-position led to a two- to three-fold increase in the anti-HIV activity compared with compound **1a** (Table 1). This improvement was duplicated by the modification of benzo[4,5]isothiazolo[2,3-*a*]pyrimidine derivatives at the 8-position (**2b**, **2c**, **2d** and **2f**), which is the equivalent position of the 9-position in pyrimido[1,2-*c*][1,3]-benzothiazin-6-imine. Similarly, introduction of acetamido group at the equivalent positions resulted in a complete loss of the anti-HIV activity of both the PD 404182 derivative (**1e**) and isothiazolopyrimidine derivative (**2e**). Furthermore, a complete loss of anti-HIV activity was observed by the introduction of the 8-bromo and 7-bromo groups to the parent compounds (**1g** and **2g**, respectively). These similar structure–activity relationships implied that the same target molecule(s) or mechanism(s) of action could possibly be involved in the anti-HIV activities of PD 404182 and the isothiazolopyrimidine derivatives.

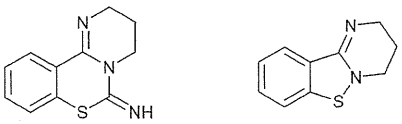

**1a** (PD 404182)
[$EC_{50}$ = 0.30 ± 0.06 μM]



**2a**
[$EC_{50}$ = 0.29 ± 0.09 μM]

Fig. 1 Structures of PD 404182 (**1a**) and benzo[4,5]isothiazolo[2,3-*a*]-pyrimidine (**2a**).

In addition, heterocyclic compounds **1a** and **2a** both inhibited early-stage HIV infection including virus attachment and membrane fusion to host cells as exemplified in comparison with DS 5000 (adsorption inhibitor)[12] and enfuvirtide (fusion inhibitor).[13] Although it was suggested that the antiviral effects of compound **1a** are derived from its virucidal effect against viral particles,[14] its antiviral mechanism of action has not yet

[a]*Graduate School of Pharmaceutical Sciences, Kyoto University, Sakyo-ku, Kyoto 606-8501, Japan. E-mail: soishi@pharm.kyoto-u.ac.jp, nfujii@pharm.kyoto-u.ac.jp; Fax: +81-75-753-4570; Tel: +81-75-753-4561*

[b]*Institute for Virus Research, Kyoto University, Sakyo-ku, Kyoto, 606-8507, Japan*

† Electronic supplementary information (ESI) available. CCDC 1037500. For ESI and crystallographic data in CIF or other electronic format see DOI: 10.1039/c5ob00301f

Table 1 Comparison of the structure–activity relationships of PD 404182 derivatives and benzo[4,5]isothiazolo[2,3-*a*]pyrimidines

| Cmpd | | $EC_{50}$ [a,7,8] (μM) | Cmpd | | $EC_{50}$ [b,11] (μM) |
|---|---|---|---|---|---|
| | 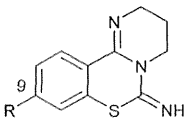 | | | 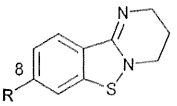 | |
| 1a (PD 404182) | R = H | 0.44 ± 0.08[c] | 2a | R = H | 0.29 ± 0.09 |
| 1b | R = Ph | 0.24 ± 0.04 | 2b | R = Ph | 0.30 ± 0.10 |
| 1c | R = *m*-anisyl | 0.15 ± 0.05 | 2c | R = *m*-anisyl | 0.10 ± 0.03 |
| 1d | R = Br | 0.25 ± 0.09[c] | 2d | R = Br | 0.22 ± 0.07 |
| 1e | R = NHAc | >10 | 2e | R = NHAc | >10 |
| 1f | 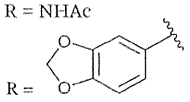 | 0.15 ± 0.03 | 2f | 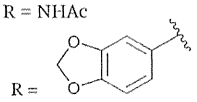 | 0.16 ± 0.02 |
| 1g | 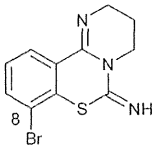 | >10[c] | 2g | 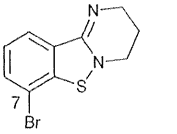 | >10[d] |

[a] $EC_{50}$ values represent the concentration of the compound required to inhibit the HIV-1 infection by 50%. The data were obtained from three independent experiments by the MAGI assay. [b] $EC_{50}$ values were obtained by the NCK assay. [c] $EC_{50}$ values were obtained by the NCK assay, compound **1a**: 0.30 ± 0.06 μM; compound **1d**: 0.14 ± 0.02 μM; compound **1g**: >10 μM. [d] Cytotoxicity was observed at 10 μM.

been sufficiently detailed. In the current study, we investigated the chemical transformations of pyrimido[1,2-*c*][1,3]benzothiazin-6-imine derivatives **1** and benzo[4,5]isothiazolo[2,3-*a*]pyrimidine derivatives 2 under the bioassay conditions.

## Results and discussion

### Synthesis

PD 404182 derivatives **1** and benzo[4,5]isothiazolo[2,3-*a*]pyrimidine derivatives 2 were synthesized according to the protocols in our previous studies (Scheme 1).[7,8,11] 2-(2-Mercaptophenyl)tetrahydropyrimidine derivatives **4** were obtained by trifluoroacetic acid (TFA)-mediated ethanolysis of the imino group in pyrimido[1,2-*c*][1,3]benzothiazin-6-imines **1**. The alternative route *via* alkaline hydrolysis of pyrimido[1,2-*c*][1,3]-benzothiazin-6-thione **3** also generated thiophenol derivatives **4**. Some thiophenol derivatives **4** could be isolated as stable crystals, such as 2-(2-mercaptophenyl)-, 2-(4-bromo-2-mercaptophenyl)- or 2-(3-bromo-2-mercaptophenyl)-tetrahydropyrimidine (**4a**, **d**, **g**). Thioanisole derivative 7 was obtained by the oxidative amidination of the corresponding benzaldehyde **5**.[15,16] Sulfuric acid-mediated deprotection of *N*-tosylated tetrahydropyrimidine **8**, derived from benzaldehyde **6** by the identical protocol,[7] afforded aniline derivative **9**.

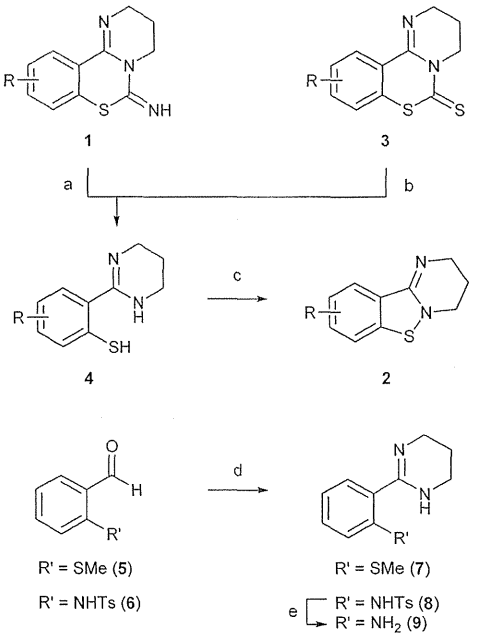


Scheme 1 Synthesis of benzo[4,5]isothiazolo[2,3-*a*]pyrimidine and 2-phenyl-1,4,5,6-tetrahydropyrimidine derivatives. Reagents and conditions: (a) TFA, $CHCl_3$–EtOH or EtOH, rt; (b) NaOH, MeOH–$H_2O$, reflux; (c) PIDA, $CHCl_3$ and/or EtOH, rt; (d) 1,3-propanediamine, $I_2$, $K_2CO_3$, *t*-BuOH, 70 °C; (e) conc. $H_2SO_4$, 100 °C.

### Identification of the inactive ingredient by transformation from PD 404182 in aqueous media

Recently, Chamoun-Emanuelli *et al.* reported that the antiviral activity of PD 404182 (**1a**) disappeared during storage under some conditions (for example, in Dulbecco's phosphate-buffered saline (pH 7) at 42 °C).[10] During our studies on PD 404182 derivatives, we also found that the anti-HIV activity from the stock solution of **1a** in DMSO was often attenuated. X-ray crystallography of the predominant component from **1a** revealed that the resulting product was 3,4-dihydro-2*H*,6*H*-

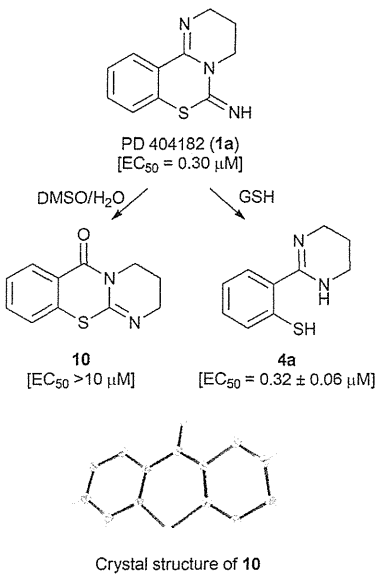


Fig. 2 Transformations of PD 404182 under assay conditions and under reductive conditions in the presence of GSH at 37 °C. $EC_{50}$ values represent the concentration of the compound required to inhibit the HIV-1 infection by 50%. The data were obtained from three independent experiments by the NCK assay.

benzo[*e*]pyrimido[2,1-*b*][1,3]thiazin-6-one **10** (Fig. 2). An apparent rearrangement of the cyclic amidine substructure in **1a** provided pyrimidothiazinone **10** with no anti-HIV activity. In contrast, benzo[4,5]isothiazolo[2,3-*a*]pyrimidine **2a** was stable in acidic and basic solutions, and the assay medium containing fetal calf serum.

### Transformation of PD 404182 and benzo[4,5]isothiazolo[2,3-*a*]-pyrimidine derivatives under reductive conditions in the presence of GSH

We investigated the conversion of PD 404182 (**1a**) in the presence of high glutathione (GSH) concentrations that mimic the intracellular environment.[17] Interestingly, the imino group of **1a** decomposed in 10 mM GSH solution at 37 °C, and was converted into thiophenol **4a** within 1 h (Fig. 2 and 3).[18] This thiophenol derivative **4a** exhibited equipotent anti-HIV activity as the parent compound **1a** ($EC_{50}$ = 0.32 ± 0.06 μM). The mechanism of conversion from **1a** into thiophenol **4a** could be *via* the release of cyanylated glutathione, which was detected by ESI-MS analysis.[19]

Our previous structure–activity relationship study of **1a** demonstrated that the 6-imino group and the 7-sulfur atom in **1a** were indispensable for the anti-HIV activity (Table 2).[7] For example, substitution of the imino group in compound **1a** with a carbonyl (**13**) or thiocarbonyl (**3a**) group resulted in a significant decrease or loss of activity. Neither pyrimido[1,2-*c*]-[1,3]benzoxazines (**14a–c**) nor pyrimido[1,2-*c*]quinazolines (**15a–c**) exhibited anti-HIV activity (Table 2). In the presence of GSH, the carbonyl (**13**) and thiocarbonyl (**3a**) derivatives were slowly converted to compound **4a** in 26 and 15% yield, respectively, after 24 h (Table 2, Fig. 3). This is in contrast with the rapid and quantitative conversion from **1a** within 1 h, indicating that a more reactive imino group in **1a** was a prerequisite for the efficient generation of **4a** with potent anti-HIV activity. In the absence of GSH, compound **13** was converted into **4a** in only 5% yield for 24 h, and **3a** did not produce **4a**, indicating that degradation of **13** and **3a** was mainly mediated by GSH.[20] Compound **14a** was unstable in the presence or absence of GSH to give a cyclic carbamate **14b** and a phenol derivative **16**,[7,21] which showed no anti-HIV activity. The carbamate **14b** and thiocarbamate **14c** were also degraded into an inactive phenol **16** in 78 and 71% yield, respectively, in GSH solution over 24 h. The pyrimido-[1,2-*c*]quinazolines (**15a–c**) were stable under identical conditions, and thus, did not produce the possible aniline **9**. In light of these results, the absent or diminished anti-HIV activity of **3a** and **13–15** is likely attributable to decreased conversion to the potent thiophenol **4a** or the poor anti-HIV activity of the parent compounds and ring-opened products.

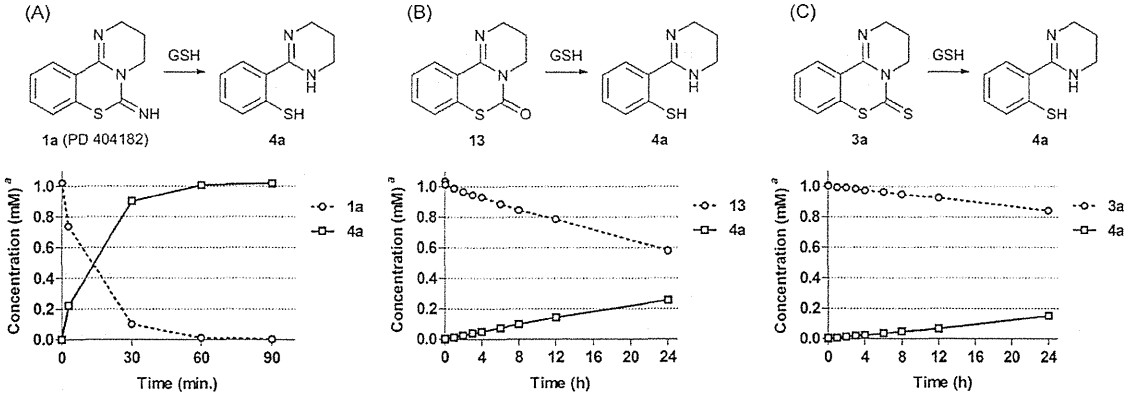


Fig. 3 Transformation of compounds **1a** (A), **13** (B) and **3a** (C) under reductive conditions in the presence of GSH. [a] The concentrations of compounds were calculated by HPLC analysis using previously determined calibration curves.